



A review on physical and data-driven modeling of buildings hygrothermal behavior: Models, approaches and simulation tools



Mohamed-Ali Hamdaoui^a, Mohammed-Hichem Benzaama^{a,*}, Yassine El Mendili^a, Daniel Chateigner^b

^a COMUE Normandie Université, Laboratoire ESITC, 1 Rue Pierre et Marie Curie, Epron 14610, France

^b Normandie Université, CRISMAT UMR CNRS n°6508, ENSICAEN, IUT Caen, Université de Caen Normandie, 6 boulevard Maréchal Juin, Caen 14050, France

ARTICLE INFO

Article history:

Received 1 June 2021

Revised 27 July 2021

Accepted 10 August 2021

Available online 14 August 2021

Keywords:

Heat, Air and moisture transfer (HAM)

Hygrothermal simulation tools

Artificial Neural Network

Machine learning

Building energy

Hygroscopic

ABSTRACT

The hygrothermal simulation of hygroscopic building materials is a real challenge, in terms of regulations and labelling, but also in decision-making. Today, we lack reference models for the hygrothermal behavior of a whole building. A scoping literature review is conducted to provide an overview of current state-of-the-art methods in order to address of these simulation methods. The most comprehensive studies are selected and examined in detail. These include physical models (White-box), which focus on solving equations that simulate the hygrothermal behavior of buildings, and data driven models, which involve implementing a prediction model using machine learning techniques (Black-box). On one hand, the white-box models are reviewed according to a two-category classification: CFD and Nodal approaches. On the other hand, the principal model used for black-box models is neural network models. The study highlights the need for a recognized method for hygrothermal simulations of hygroscopic envelopes. It provides a better understanding of the hygrothermal simulation, which helps to choose the most suitable tool or model. In addition, this review points out that there is limited application of data-driven methods to simulate the hygrothermal behavior of hygroscopic envelopes. This analysis study highlights future research gaps to overcome in order to stimulate data-driven building performance design.

© 2021 Elsevier B.V. All rights reserved.

Contents

1. Introduction	3
1.1. Background	3
1.2. Aim of the study	4
2. Methodology	4
3. Understanding of hygrothermal transfers in buildings	4
3.1. Characteristic of hygroscopic low carbon material	4
3.2. Heat and moisture transfer in hygroscopic material	6
3.2.1. Moisture transports in porous media	6
3.2.2. Thermal diffusion in porous media	7
3.2.3. Different methods for heat, air and moisture (HAM) modeling	7
3.2.4. Mathematical models of coupled heat and moisture transfer in porous media	7
4. Physical modeling	8
4.1. Nodal approach	8
4.1.1. Strength of the nodal approach	9
4.1.2. Weakness of the nodal approach	9
4.1.3. Simplified models for simulating surface moisture adsorption and desorption	9
4.2. Computed fluid dynamics (CFD) approach	10
4.2.1. Strength of the CFD approach	11
4.2.2. Weakness of the CFD approach	11

* Corresponding author.

E-mail address: mohammed-hichem.benzaama@esitc-caen.fr (M.-H. Benzaama).

4.3. Co-simulation of hygrothermal behavior modeling 12

4.4. Inputs for hygrothermal simulation tools 13

 4.4.1. Geometry 13

 4.4.2. Mesh generation 13

 4.4.3. Material properties 14

 4.4.3.1. Sorption isotherm 14

 4.4.3.2. Hysteresis effect 15

 4.4.4. Boundary and initial conditions 16

5. Statistical methods using machine learning 18

 5.1. Artificial neural networks modeling 18

 5.2. Artificial neural networks principles 18

 5.3. Artificial neural networks architectures 18

 5.3.1. Learning methods in ANN 19

 5.3.2. Statistical comparison and error-correction 20

 5.4. ANN approach for building energy simulation 20

6. Existing data for validation 21

7. Conclusion 22

 Declaration of Competing Interest 22

 References 22

Nomenclature

A_i	actual measured/experimental data (-)	H_w	enthalpy of water liquid phase (J kg ⁻¹)
b_j	bias weight at layer level j (-)	j_l	volume flow density of moisture liquid diffusion (m ³ m ⁻² s ⁻¹)
c	energy constant for the specific heat of sorption (-)	j_v	mass flow density of moisture vapor diffusion (kg m ² s ⁻¹)
C	the volumetric heat capacity	j_w	flow density of water content (m ³ m ⁻² s ⁻¹)
c_0	entropic adjustment factors (-)	k_0	entropic adjustment factors (-)
c_g	adsorption constant of GAB model (-)	K_b	boltzmann constant (kg m ² s ⁻² K ⁻¹) or (J K ⁻¹)
c_p	specific heat of dry material (J kg ⁻¹ K ⁻¹)	K_g	adsorption constant of GAB model (-)
C_v	molar concentration of vapor (mol m ⁻³)	K_h	hydraulic conductivity (m s ⁻¹)
d	pore diameter (m)	K_p	permeability (m ²)
D_b	bound water diffusivity (m ² min ⁻¹)	K_w	liquid water permeability (kg m ⁻¹ s ⁻¹ Pa ⁻¹)
D_c	molecular diffusion coefficient proportional to the mean free path (m ² s ⁻¹)	L_v	latent heat of evaporation (J kg ⁻¹)
D_K	knudsen diffusion coefficient proportional to the pores size (m ² s ⁻¹)	m_a	mass of air particle (kg)
D_m	moisture diffusion coefficient of the porous media (m ² s ⁻¹)	m_{rain}	mass flux for rain (kg m ⁻² s ⁻¹)
D_T	moisture diffusion coefficient related to the temperature gradient (m ² s ⁻¹ K ⁻¹)	m_w	mass flux for liquid water (kg m ⁻² s ⁻¹)
$D_{T,liq}$	liquid diffusion coefficient related to the temperature gradient (m ² s ⁻¹ K ⁻¹) or (kg m ⁻¹ s ⁻¹ K ⁻¹)	N_c	rate of moisture molecular diffusion (mol m ⁻² s ⁻¹)
$D_{T,vap}$	vapor diffusion coefficient related to the temperature gradient (m ² s ⁻¹ K ⁻¹) or (kg m ⁻¹ s ⁻¹ K ⁻¹)	N_K	rate of moisture diffusion (Knudsen effusion) (mol m ⁻² -s ⁻¹)
D_v	water vapor diffusivity (m ² min ⁻¹)	P	pressure (Pa)
D_w	moisture water diffusion coefficient (m ² s ⁻¹)	p_0	constant atmospheric air pressure (Pa)
D_0	moisture diffusion coefficient related to the moisture gradient (m ² s ⁻¹)	p_c	suction pressure (Pa)
$D_{0,liq}$	liquid diffusion coefficient related to the moisture gradient (m ² s ⁻¹)	P_i	predicted network output (-)
$D_{0,vap}$	vapor diffusion coefficient related to the moisture gradient (m ² s ⁻¹)	p_l	liquid pressure (Pa)
D_ϕ	liquid conduction coefficient (kg m ⁻¹ s ⁻¹)	p_{sat}, p_{vap}	water vapor saturation pressure (Pa)
E	phase conversion number (-)	$Q_{rad,int}$	internal source radiation (W m ⁻²)
f	dimensionless diffusivity tensor (-)	$Q_{rad,sky}$	radiative heat transfer term (W m ⁻²)
h	capillary pressure (m)	R	ideal gas constant (J mol ⁻¹ K ⁻¹)
H_0	molar sorption enthalpies of the monolayer (J mol ⁻¹)	S_ϕ	source term (W m ⁻³)
H_b	enthalpy of bound water (J kg ⁻¹)	T	temperature (K)
$h_{c,ext}$	convective heat exchange coefficient of the exterior surface (W m ⁻² K ⁻¹)	T_i	indoor air temperature (K)
$h_{c,int}$	convective heat exchange coefficient of the interior surface (W m ⁻² K ⁻¹)	$T_{surrounding}$	average surface temperature of all surfaces in an area (K)
$h_{r,int}$	radiative heat exchange coefficient of the interior surface (W m ⁻² K ⁻¹)	u	relative moisture concentration (kg kg ⁻¹)
H_s	enthalpy of water solid phase (J kg ⁻¹)	u_a	absorption moisture content corresponding to current RH-Value (kg kg ⁻¹)
h_v	evaporation enthalpy of water (J kg ⁻¹)	u_{ads}	main curves of the adsorption (kg kg ⁻¹)
		u_d	desorption moisture content corresponding to current RH-Value (kg kg ⁻¹)
		u_{des}	main curves of the desorption (kg kg ⁻¹)
		u_j	linear combiner output due the input signals
		u_r	residual moisture contents of the scanning curve (kg kg ⁻¹)

u_s	saturated moisture contents of the scanning curve (kg kg ⁻¹)	θ_u	water content at the meeting point of the two boundary curves (m ³ m ⁻³)
V	velocity vector (m s ⁻¹)	θ_w	water content on the boundary wetting curve at suction (m ³ m ⁻³)
v_j	induced local field (-)	λ	thermal conductivity (W m ⁻¹ K ⁻¹)
V_w	liquid phase velocity (m min ⁻¹)	M	dynamic viscosity of liquid (Pa s)
W	moisture content (m ³ m ⁻³)	ζ_a	absorption moisture capacity at the current relative humidity (kg kg ⁻¹)
$w_{i,j}$	synaptic weights of the neuron (-)	ζ_d	desorption moisture at the current at the current relative humidity (kg kg ⁻¹)
W_r	total of all radiative heat sources in the volume area (W)	ζ_{hys}	moisture capacity at hysteresis (kg kg ⁻¹)
W_v	vapor mass fraction (-)	ρ	density (kg m ⁻³)
X	mass moisture content (Kg Kg ⁻¹)	ρ_s	density of water solid phase (kg m ⁻³)
X_0	monolayer moisture content (m ³ m ⁻³) or (kg kg ⁻¹)	ρ_v	density of water vapor phase (kg m ⁻³)
x_n	input signal (-)	ρ_w	density of water liquid phase (kg m ⁻³)
y_j	output signal of the neuron (-)	τ_{rm}	moisture propagation in a capillary porous media (s)
<i>Greek</i>		φ	relative humidity (-)
α	thermal diffusion coefficient (m ² s ⁻¹)	$\varphi(x)$	activation function (-)
β_v	convective mass transfer coefficient (kg m ⁻² s ⁻¹ Pa ⁻¹)	ϕ	standard physical parameter (-)
Γ_ϕ	diffusion coefficient for the standard physical parameter (m ² s ⁻¹)		
δ	thermogradient coefficient (K ⁻¹)		
δ_p	water vapor permeability (kg m ⁻¹ s ⁻¹ Pa ⁻¹)		
ε_b	volume fraction of liquid (-)		
ε_s	volume fraction of solid (-)		
ε_v	volume fraction of vapor (-)		
θ_d	water content on the boundary drying curve at suction (m ³ m ⁻³)		
θ_r	residual moisture content (m ³ m ⁻³)		
θ_s	saturated moisture content (m ³ m ⁻³)		
		<i>Abbreviations</i>	
		R^2	coefficient of determination (-)
		RMSE	Root Mean Square Error (-)
		SSE	Sum of Square Error (-)
		SSR	Sum of Squares Regression (-)
		SST	Sum of Squares Total (-)

1. Introduction

1.1. Background

The reduction of fossil-based energy use, mainly in the construction field, is of considerably large importance in research. In 2017, world energy usage in the buildings sector accounted for 21% [1] of the global total final consumption, ranking third behind the industry and transport sectors. Additionally, 9% [1] of global total final consumption energy was also dissipated and never used. As a consequence, the buildings field rose energy consumption over the past decades, calling for more power production and, as a result, CO₂ emissions.

In the last three decades, especially after the United Nations' publication of Our Common Future [2], in 1987, also known as the Brundtland Report, climate policy around the globe has begun to change radically. This last one focuses on a sustainable development way that protects the ecosystem and the climate, as well as bringing global environmental and development challenges into the formal worldwide nation concerns. As a result, in 1992, the United Nations Framework Convention on Climate Change (UNFCCC) [3] was signed to address the major challenges to the world's climate and economic growth, especially in sectors that consume a lot of energy, such as buildings. Thus, many attempts have been made at the international and national levels, such as in Europe, to preserve ecosystem equilibrium and sustainability with the aim of making them stable and efficient. Although, many nomenclatures of international conventions and protocols were elaborated to categorize these efforts, such as the establishment of the Montréal and Kyoto Protocols in 1987 [4] and 1997 [5] respectively, followed by the Paris agreement which became effective in 2016 [6]. One of their goals is to keep greenhouse gas levels stable at a scale that protects biodiversity and allows the environment to respond to climate change in a conventional manner.

There are currently several new trends that are adopted in order to reduce high greenhouse gas emissions and minimize energy use, notably in the buildings sector, which is the second largest energy consumer in the European Union, accounting for up to 26.1% of total energy consumption [7]. More precisely, building space heating accounts for about 63.6% [8] of the overall energy demand in the residential building sector.

Consequently, in order to counter both energy consumption and greenhouse gas emission increases, two main trends are recently developed: the enhancement of the insulation efficiency of the building structure envelope and thereby reducing energy consumption, and the elaboration of new low carbon materials, to reduce carbon dioxide footprint. Such tendencies can be accompanied and achieved through alternative materials such as aerated concrete [9,10], hemp concrete [11–15] and bio-based material [16,17] as natural fiber components, straw and rammed earth which are often referred to those as porous materials.

The main advantage of such porous materials, directly coming from the use of natural fibers and incorporation of air, is the resulting lower thermal conductivity compared to denser concretes. However, porousness comes along usually with mechanical strength decrease, and an acceptable balance between mechanical and thermal properties must be achieved. Once this mechanical-thermal equilibrium satisfied, as a result of the higher porosity and tortuosity, buildings have the capacity to trap moisture, and potentially release it depending on climatic and outside conditions. These latter behaviors may also influence the measurements and simulations of the whole building energy needs [18] and have to be taken into account.

The dynamic energy simulation of such a building construction type is a real challenge, in terms of regulations and labelling but also for decision making (Implementation, materials choice, architectural design, retrofit . . .). Today, we lack reference modeling of the transient hygrothermal behavior of this envelope type. In addi-

tion, there is no model yet concerning the impact of coupled heat and mass transfer phenomena on the global energy performance of this building construction type. In recent decades, there has been an increasing in demand for simulation methods to calculate the coupled heat and moisture transfers of building components and envelopes [19]. It would also be very advantageous to determine the hygrothermal performances of using more ecologic hygroscopic materials or the impact of various climate conditions on potential low-carbon buildings.

Building energy simulation (BES) and computational fluid dynamics (CFD) are two of the many numerical simulation approaches used in the building sector to calculate the energy balance needs. Where BES approach stands for a single mass model that estimates physical parameters in a single node, the profile of those parameters is uniform across the given region, allowing for a long-term unsteady analysis to be considered. The CFD approach, on the other hand, focuses on the numerical meshing of the entire building volume into small elements or volumes, which results in a large computing load, particularly for unsteady states simulations, but it can be combined with the BES approach.

Therefore, significant initiative using various models and approaches in the building sector is essential to predict future potential improvements. These require energy calculation by which incorporate efficient computing methods into building simulation tools while taking into account peculiar aspects as the coupled heat and moisture transfer through the envelope. As a consequence, scientists and engineers use a wide range of simulation techniques, depending on the use cases [20–24]. An accurate hygrothermal model is essential to improve and evaluate energy performance. Actually, two types of models can be distinguished:

- White-box models which are based on physical knowledge of the system and energy balance equations. These are often obtained through energy simulation software such as TRNSYS, EnergyPlus, WUFI, COMSOL Multiphysics...
- Black-box models which use only measured input/output data and statistical estimation methods such as Artificial Neural Networks (ANN), without physics-based models.

However, each technique has its own advantages and drawbacks. M. H. Benzaama et al. [25] worked out a comparative study between these different models. Their conclusions are:

- For white-box models such as TRNSYS tools: (i) such models often require a great large set-up and computation time. (ii) involve a lot of inputs to define the model, such as the composition of the building envelope. In some studies, it is difficult, if not impossible, to recover this input.
- For black-box models like ANN, thermal performance predictions based on available data, preferably large datasets, with genetic and machine learning methods are necessary. After calculations, it is difficult to understand the physical phenomena that these models depict, and the hygrothermal behavior changes related to the climatic conditions, occupant's behavior, set-point temperatures...

1.2. Aim of the study

In many simulation tools that study the energy behavior of buildings [26,27], the diffusion of moisture through the walls is not taken into account. Knowing that heat and moisture transfer can be made at the same time and coupled [28,29]. Thermal and moisture gradients can directly impact walls behavior and indoor air temperature and humidity. To our best knowledge, the simulation models developed in the literature for buildings are too simple to be used for a detailed analysis of thermal comfort and there is no

published review on the hygrothermal models used for bio-based materials. These actual limitations need to be addressed in order to be able to simulate the real hygrothermal behavior of bio-based buildings for different climates, taking into account the occupants and the HVAC (Heating, Ventilation and Air-Conditioning) systems.

This paper aims at reviewing the current methodology for simulating the hygrothermal behavior of bio-based buildings. The principal objectives of this study are:

- To identify studies concerning the hygrothermal performance of hygroscopic envelopes.
- To clarify the relationship between thermal and mass transfer and discuss the approach to combine them.
- To identify potential methodological discrepancies that could explain inconsistent findings from competing hygrothermal models.
- To show the performance of hygroscopic envelopes addressed through hygrothermal simulations in the existing literature.
- To present the physical and machine learning models used in hygrothermal simulation.
- To list the numerical tools that can simulate heat and moisture transfers at the building scale.
- To demonstrate how to integrate mass transfer in dynamic thermal simulation tools.

The present paper aims to show this knowledge gap and the hygrothermal models used until now at different scales. Therefore, the physical methods used to model the buildings' hygrothermal behavior will be presented. Then, we will go through some of the machine learning techniques that are commonly used to derive a prediction model from applicable data in order to simulate temperature and humidity profiles at various building scales and different times.

2. Methodology

Following a review of the relevant existing literature, we have developed a conceptual framework that summarizes and visualizes our research methodology. We divide our working approach into three main stages (Fig. 1), each one composed of several steps, as explained in details in the following sections:

- Stage one: Understanding the hygrothermal transfer in buildings, with a focus on hygroscopic materials used in the literature and on physical grounds driving the hygrothermal behavior.
- Stage two: Presenting the physical models used in the literature, and specifying the advantages and limitations of each method.
- Stage three: A description of neural network models and their application in building hygrothermal behavior studies.

3. Understanding of hygrothermal transfers in buildings

The heat and moisture transfers in porous building materials and envelopes are strongly coupled with nonlinear mechanisms. Accurate models for coupled heat and moisture transfer in hygroscopic materials are difficult to accomplish [30]. Accordingly, before looking deeper into coupling the two behaviors, it is necessary to understand the materials used in construction that ease heat and moisture transfers, as well as the general laws and basic underlying processes.

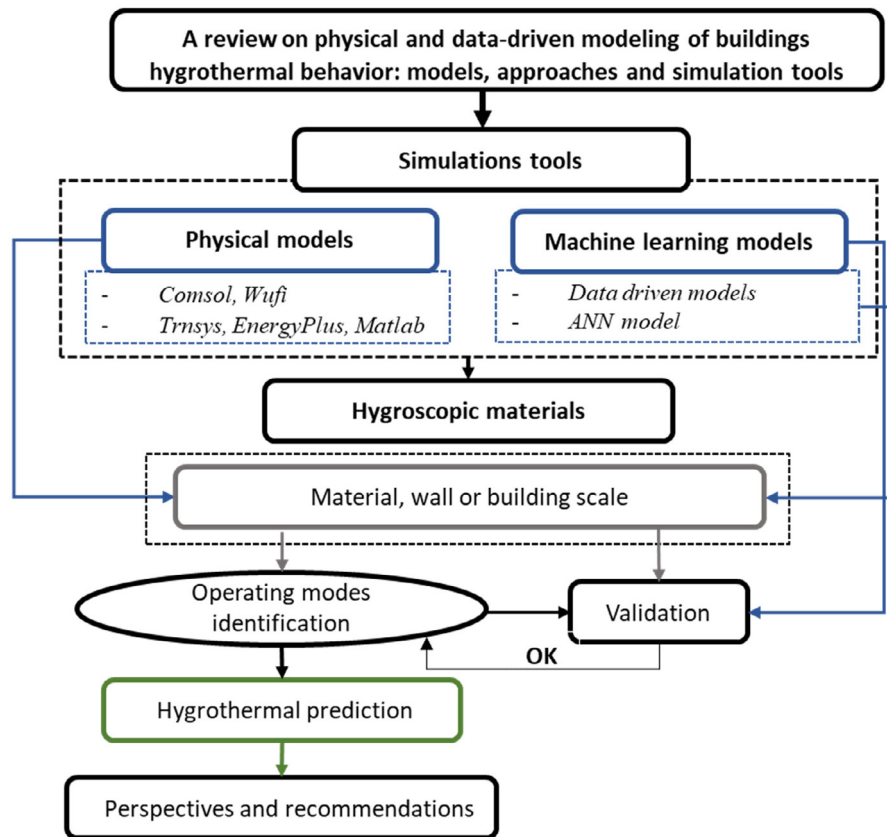


Fig. 1. Schematic overview of hygrothermal simulation approaches.

3.1. Characteristic of hygroscopic low carbon material

Low-carbon construction materials are typically sourced from bio-based or straw/rammed earth materials. They can be elaborated as mixes of quantities of high carbon inputs and industrial wastes [31], hereby largely contributing to the carbon storage and environmental preservation. For this reason, governments and public authorities encourage their use in newly developed and renovation of facilities and buildings. Therefore, a specific category of construction materials has been developed for the building sector which utilizes natural fibers [32], inducing large porosities and consequently significantly decreases their thermal conductivity. On one hand, bio-based resources can be wood, rape, straw, hemp, flax shives, cork, and rice husk ... [33]. Straw/rammed earth materials, on the other hand, are extracted from natural resources, such as raw earth or dry stones. In construction industry, these materials are used for framing, insulation, supporting composite structures, mortars. They come in a variety of items such as panels, beams, vegetal concrete blocks, rolls, bulk, bricks ... and eventually mixed with other materials from industry. Examples of hygroscopic materials used in previous research can be classified (Table 1) relative to their functionalization and resource type.

Raw/rammed earth materials have been used for buildings over hundreds of years [40]. Some of the advantages of their use include the fact that they respond well to the rehabilitation needs and ameliorate the energy efficiency and interior comfort. Raw earth can be used as a building material such as bauge and crushed earth brick, or as a filling material like cob, straw earth and woodchip earth, for a wide range of construction techniques [41]. They can also be used as a layer for a supporting structure. As the bio-based/raw-earth materials exhibit high performances in terms of

thermal insulation and hygrometric comfort, thanks to their thermal dephasing and respiration properties, they have been commonly used in the construction of buildings. Also due to their permeability to water liquid and vapor, they are usually classified as hygroscopic materials [42] and as porous media. However, such materials have the ability to restore moisture, which can cause modifications in their physical properties, mainly mechanical, thermal, and hydric properties. For instance, as moisture absorption raises the thermal conductivity of insulating components [43,44], a resulting increase in heating energy consumption occurs.

Consequently, the degradation of materials is a crucial element to avoid the development of harmful uncontrolled mechanisms, affecting thus the materials. Indeed, the study of the degradation pathologies is essential to identify the most appropriate type and methods of intervention and renovation [45,46].

The causes of material degradation are attributed to both internal and external factors, i.e. the physicochemical composition of materials (microstructural properties) and their exposure to environmental actions [47]. Usually, the main causes of building material degradation are moisture, temperature, pollutants and freeze-thaw cycles [47] and their associated gradients.

Among the external factors, the problem of rising damp is largely identified as one of the main causes of building deterioration [48], which involves significant degradation processes, in particular in historic buildings [49,50] through moisture and air pollution actions on limestone degradation in historic buildings [51,52]. Climate is another relevant factor in degradation phenomena change. It also affects the occurrence of the freeze-thaw cycles and generates a mechanical stress which degrades building stone surfaces, resulting in the degradation of the building surface [53]. It is essential to understand material degradation factors such a moisture buffering in order to properly model building hygrothermal perfor-

Table 1
Various bio-based materials used in low-carbon building.

Study	Building components	Wall Thickness (mm)	Material type	Type of use
Zhang et al. [34]	Magnesium phosphate cement (MPC) and corn stalk (CS)	30 – 35	Bio-composites	Structural Wall
Reuge et al. [35]	Lime-hemp render/panel made of hemp shiv and an organic binder/ hemp flax and cotton/compressed straw/clay-hemp plaster	340	Bio-composites	Insulation Wall
Bagarić et al. [36]	Recycled aggregate concrete/Glass wool thermal insulation	420	Low carbon	Structural & insulation wall
Dong et al. [37]	Exterior coating/Wood fiberboard/Oriented Strand board Panel	80 – 177	Bio-based	Structural wall
Alioua et al. [16]	Date palm concrete (DPC)	150	Bio-composites	Structural wall
Tadeu et al. [38]	ICB (insulation cork board)/OSB (Oriented strand board)/Mortar/ concrete	78 – 255	Bio-composites	Structural & insulation wall
Moujalled et al. [14]	Hemp concrete/Lime-sand plaster	330	Bio-composites	Structural wall
Colinart et al. [13]	Hemp concrete coated with lime-based plasters	76	Bio-composites	Structural wall
Hou et al. [39]	Hollow concrete filled with compressed straw bricks	260	Bio-composites	Structural wall

mance and avoid inappropriate energy balance modeling, including the coupled heat and moisture transfer coupling at all the building scales.

3.2. Heat and moisture transfer in hygroscopic material

3.2.1. Moisture transports in porous media

Moisture refers to water transfers at both liquid and vapor states. The moisture transport in hygroscopic material is driven by a number of several mechanics that are responsible for each phase's movement (liquid and vapor) [54]. The influence of any of these mechanisms on the amount of water fixed inside and/or at materials' surfaces is highly dependent on the material's properties, like the porosity, the composition of the pores, and the condition of the pores' surface, as well as the climate to which it is exposed. These two phases of water have different transfer mechanisms [55].

Primarily, the surface adsorption of existing moisture in the ambient air or capillary condensation within the material are the most significant moisture binding phenomena [23]. For a specific hygroscopic condition and porous media, both the adsorption and capillary condensation can occur simultaneously.

For example, in the case of a porous material placed in an ambient condition, as the Relative Humidity (RH) begins to rise in regard to the hygroscopic material's initial conditions at a steady temperature value (isothermal condition), we can notice that the material begins to gain weight and adsorb the water which exists in the air [56]. We can explain that by the intervention of intermolecular Van der Waals forces on the water molecules that end up creating the previously described phenomenon [57].

The highest water content that can be reached is usually much lower than the maximum water content that can be achieved at absolute saturation. Mono-molecular adsorption occurs at low relative humidity margins, generally less than 20%, which corresponds to the retention of a one single layer of water molecule on the pore's surfaces (Langmuir theory) [58]. When the relative humidity is above 50%, Multi-molecular adsorption occurs, which describes the fixation of several layers on the first one (BET theory) [59]. For small enough pore diameters and RH values larger than 50%, multi-molecular layers that accumulate within the pores, can have the potential to be combined. At this stage, a meniscus forms a liquid bridge by separating the liquid phase from the vapor phase. At a relative humidity of less than 100%, a liquid phase and a vapor phase are in equilibrium within the pores, giving rise to capillary condensation within the hygroscopic material. For this purpose, the description of the vapor and liquid phase is given as follows:

- Vapor phase

As far as moisture transfer under the phase vapor is considered [60–62], it is interesting to note that the possibility of water mole-

cule collisions in the inside pore surfaces of the hygroscopic material is greater in large pores than in small pores, This occurs because shock against other molecules is much weaker than shock against solid surfaces. In this instance, the water vapor molecule's mean free path represents the actual distance of displacement covered by the water small particle between two molecular shocks [63]. Thus, two scenarios can be imagined based on the pore size and molecular density. First, molecular diffusion can be used to describe vapor transfer in pores with a radius greater than the mean free path. Second, the Knüdsen effusion is the transfer of vapor through pores with a radius smaller than the mean free path [64]. At the pore scale, Fick's law (1855) can describe the molecular diffusion phenomenon when the pore size is larger than the mean free path. Under the hypothesis of a perfect gas and a constant total pressure:

$$N_c = -D_c \nabla C_v \tag{1}$$

Where N_c is the rate of molecular moisture diffusion, D_c is the molecular diffusion coefficient proportional to the mean free path, and C_v is the molar concentration of vapor.

For the same purposes as molecular diffusion, the Knüdsen effusion phenomenon occurs in pores with a radius smaller than the mean free path. Therefore, molecules' interactions dissipate, and their speed is affected by collisions. In this case, the diffusion coefficient is proportional to the pore radius rather than the mean free direction.

$$N_K = -D_K \nabla C_v \text{ and } D_K = \frac{d}{3} \sqrt{\frac{8K_b T}{\pi m_a}} \tag{2}$$

Where N_K is the rate of moisture diffusion, D_K is the Knüdsen diffusion coefficient proportional to the pores size, C_v is the molar concentration of vapor, d is the pore diameter, K_b is the Boltzmann constant, T is the absolute temperature of the gas, and m_a is the mass of air particle.

- Liquid phase

Moisture transfer by the liquid phase [15,29,38], is operated either by the forces due to capillary pressure gradients during the adsorption or desorption processes, or by gravity forces [23]. However, it is often transported in the decreased pressure direction. Therefore, by neglecting the gravity forces, the Darcy's law can describe the liquid flux density:

$$j_l = -\frac{k_p}{\mu} \nabla p_l \tag{3}$$

Where j_l is the volume flow density of moisture liquid diffusion, K_p is the permeability, μ is the dynamic viscosity of liquid and p_l is the liquid pressure. With $p_c = p_l - p_0$, and according to the law of Laplace, where p_c is the suction pressure and p_0 is the atmospheric

air pressure, the equation above can be written as a function of moisture water content,

$$j_w = -D_w \nabla w \tag{4}$$

Where j_w is the flow density of water content, D_w is the moisture water diffusion coefficient and w is the moisture water content.

3.2.2. Thermal diffusion in porous media

Heat transfer can be described as a change in the enthalpy of a material caused by a change in temperature. This variation is often due to a number of reasons. First, the heat flux density gradient is directly proportional to the temperature gradient, as defined by Fourier's law, and to the conductivity of the material. Second, the heat flux gradient can also be transported by the moisture flux, defined as a source term in the general heat equation [30]. When working with continuous media, this phenomenon is often neglected. But it can be considered when working with porous media by including it as a source term when dealing with hygroscopic materials that are permeable to moisture adsorption. As a result, the heat transfer equation is as follows:

$$\rho c_p \frac{\partial T}{\partial t} = \nabla(\lambda \nabla T) + \nabla(L_v \nabla j_v) \tag{5}$$

Where ρ is the density of material, c_p is the specific heat of the dry material, λ is the thermal conductivity of material, L_v is the latent heat of evaporation and j_v is the mass flow density of moisture vapor diffusion. In the general form of the heat transport equation for porous media, only the energy of the vapor phase change is considered, with liquid diffusion being neglected.

3.2.3. Different methods for heat, air and moisture (HAM) modeling

Energy and mass conservation transport equations can be used to explain heat and mass transfers through building envelopes. Heat flux by conduction, convection, and radiation are quantified in energy balance equations [65]. Moisture transfer by vapor diffusion, moisture convection, and liquid transfer are considered in mass balance equations, whereas air-moisture convection can be entrained by natural, external, or mechanically forced air flows [66].

The interactions of these phenomena is identified as the Heat, Air, and Moisture transfer phenomena (HAM), which is important for any whole building envelope hygrothermal balance study [67]. The Fig. 2 illustrates the physical interactions in place between the various components of the building indoor atmosphere and envelope.

There are numerous computer-based methods for predicting building hygrothermal behavior in the literature. The sophistication of these models varies considerably in terms of their underlying mathematical and physical descriptions. This complexity is determined by the degree to which the model considers the following parameters: Dimensions of the heat and moisture transports (1D, 2D or 3D), physical model regime (steady-state, quasi-static, or unsteady), knowledge and availability of different details,

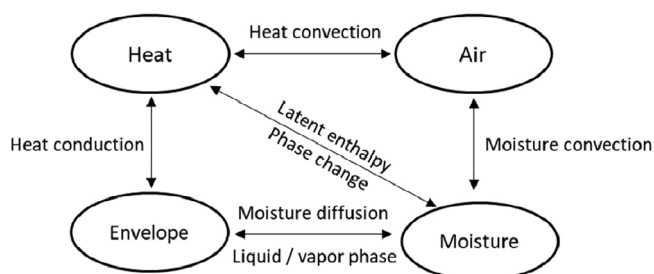


Fig. 2. Different form of physical interaction between the building envelope and the heat, air and moisture.

such as, material properties, temperature, building size, and climate conditions. All the hygrothermal simulation tools that will be discussed later in this paper are dependent on a number of methods, such as physical and mathematical computational approaches. These can use the finite difference, finite volume or finite element methods to solve numerically the physical problem. There is also the statistical method known as the Artificial Neural Network (ANN) approach based on machine learning techniques is added to the discussion.

3.2.4. Mathematical models of coupled heat and moisture transfer in porous media

The principles of mass and energy conservation are used to develop heat and moisture transfer models. The driving forces for moisture movement are the common factors between the different hygrothermal models for porous building envelopes and materials. Moisture content, capillary pressure, partial water vapor pressure, relative humidity, and air moisture content are some of the moistures driving forces used in current hygrothermal models. We present below the most used models:

- Philip and De Vries model

In 1957, Philip and De Vries developed the first coupled heat and moisture models. It was developed on the basis of their hypothesis of moisture transport in the soil as in function of temperature [20]. The volumetric water content θ and the temperature T are the main transport's driving forces for heat and moisture transfer, where their general differential equation for the transport of moisture in porous media, is written as:

$$\frac{\partial \theta}{\partial t} = \nabla(D_\theta \nabla \theta) + \nabla(D_T \nabla T) + \frac{\partial K_h}{\partial z} \tag{6}$$

$$D_\theta = D_{\theta,liq} + D_{\theta,vap} \tag{7}$$

$$D_T = D_{T,liq} + D_{T,vap} \tag{8}$$

Where D_T and D_θ are respectively the moisture diffusion coefficient related to the temperature gradient and the moisture gradient, also D_{liq} and D_{vap} are the moisture diffusion coefficient related respectively to the moisture transfers in liquid and vapor phase respectively and k_h is the hydraulic conductivity which generally related to the gravity forces. The heat transfer equation is written as:

$$C \frac{\partial T}{\partial t} = \nabla(\lambda \nabla T) - L_v \nabla(D_{\theta,vap} \nabla \theta) \tag{13}$$

Where C is the volumetric heat capacity, λ is the thermal conductivity and $D_{\theta,vap}$ is the vapor diffusion coefficient related to the moisture gradient. In Philip and De Vries' heat conduction equation, the energy of vapor diffusion is the only heat term that was properly considered.

- Luikov Model

In 1966, Luikov suggested a model focusing on the thermodynamics of irreversible systems for isothermal and non-isothermal processes. This model was founded on a powerful descriptive study for the prediction of heat and moisture transfer in capillary porous media at the macroscopic scale [22]. The driving forces of the coupled heat and moisture transfer are relative moisture concentration u and the temperature T . The moisture transport equation for porous media can be written as follows under non-isothermal conditions:

$$\frac{\partial u}{\partial t} + \tau_{rm} \frac{\partial^2 u}{\partial t^2} = D_m \nabla(\nabla u + \delta \nabla T) \tag{14}$$

Where, τ_{rm} is the time of moisture propagation in the capillary porous media, D_m is the moisture diffusion coefficient of the porous media and δ is the thermogradient coefficient. The additional term on the right-hand side of the equation, which characterizes moisture capillary actions, distinguishes this model from ordinary moisture modeling. For porous media, the heat transfer equation is written as:

$$\frac{\partial T}{\partial t} = \alpha \cdot \nabla(\nabla T) + \frac{E}{c_p} L \frac{\partial u}{\partial t} \quad (15)$$

Where, α is the thermal diffusion coefficient ($\lambda/\rho \cdot c_p$), E is the phase conversion number and L is the latent heat of evaporation.

- Whitaker model

In 1977, Whitaker proposed a more detailed theory in which transport equations are described for each phase (solid, liquid and gas) in macroscopic and microscopic levels based on the local average volume behavior [21]. This theory is based on a model with two dependent variables, moisture X and temperature T . The differential equation for moisture is:

$$\rho_s \frac{\partial X}{\partial t} = \nabla \left(\rho_s f D_v \nabla W_v + D_b \nabla \rho_v - \rho_w \bar{V}_w \right) \quad (16)$$

Where X is the mass moisture content. ρ_v , ρ_w , ρ_s are respectively the density of water vapor, liquid phase and the solid phase, f is the dimensionless diffusivity tensor, W_v is the vapor mass fraction, D_v and D_b are respectively the water vapor and bound water diffusivity and V_w is the liquid phase velocity [68]. The differential equation of heat is shown as follow:

$$\frac{\partial(\varepsilon_w \rho_w H_w + \varepsilon_g \rho_v H_v + \varepsilon_s \rho_s H_s + \bar{\rho}_b \bar{H}_b)}{\partial t} = \nabla(\lambda \nabla T) + H_v \rho_g f D_v \nabla W_v + H_b D_b \nabla \rho_v - H_w \rho_w \bar{V}_w \quad (17)$$

Where H_w , H_v , H_s and H_b are respectively the enthalpy of the liquid phase, vapor phase, solid phase of water and enthalpy of bound water. ε_b , ε_v , and ε_s are respectively the volume fraction of liquid, vapor and solid, and λ is the thermal conductivity of the porous media [68].

- Künzel model

In 1995, Künzel introduced a new model that was quite similar to those developed in previous decades, but it was based on Kieβl's theorem. In this paradigm, Künzel attempted to use the terms of relative humidity ϕ and temperature T as the primary driving forces to describe the coupled heat and moisture transfer in building components [23].

$$\frac{dw}{d\phi} \frac{\partial \phi}{\partial t} = \nabla(D_\phi \nabla \phi + \delta_p \nabla(\phi p_{sat})) \quad (18)$$

Where ($dw/d\phi$) is the moisture storage capacity of the porous material, D_ϕ is the liquid conduction coefficient, δ_p is the water vapor permeability of the porous material, ϕ is the relative humidity and p_{sat} is the water vapor saturation pressure. The Künzel model for heat transfers writes:

$$\frac{dH}{dT} \cdot \frac{\partial T}{\partial t} = \nabla(\lambda \nabla T) + h_v \nabla(\delta_p \nabla(\phi p_{sat})) \quad (19)$$

Where (dH/dT) is the heat storage capacity of the porous material, λ is the thermal conductivity and h_v is the evaporation enthalpy of water.

- Mendes model

In 1999, Mendes proposed a new hygrothermal model based on Philip and De Vries' equations, but he instead used the volumetric moisture content θ and the temperature gradient T as the principle driving forces for the coupled heat and moisture transfer equations [24]. The current model of moisture transfer equation is written as follows:

$$\frac{\partial \theta}{\partial t} = \nabla(D_T \nabla T + D_\theta \nabla \theta) \quad (20)$$

Where, θ is the volumetric moisture content, D_T and D_θ are the total moisture diffusion coefficient includes the vapor and liquid phases associated respectively to the temperature gradient and the moisture gradient. For heat transfers, Mendes proposes:

$$\rho \cdot c_p \cdot \frac{\partial T}{\partial t} = \nabla(\lambda \nabla T) + L \cdot \nabla(D_{T,vap} \nabla T + D_{\theta,vap} \nabla \theta) \quad (21)$$

Where ρ is the density of the material, c_p is the specific heat of the dry material, λ is the thermal conductivity of material, L is the latent heat of evaporation and $D_{\theta,vap}$ and $D_{T,vap}$ are the vapor diffusion coefficient associated respectively the to the moisture content and temperature gradients.

In 2002, Mendes et al. created a new methodology to solve strongly coupled heat and mass transfer equations in hygroscopic material. He was able to linearize the vapor exchange between the wall and the ambient air as a result of temperature and moisture content variations [30], which minimizes the time required to calculate the numerical solution.

4. Physical modeling

Current simulation techniques to estimate building energy behavior are founded on physical approaches that are unable to take into account all real conditions and situations. Few building simulation tools detail precisely the envelope [23,69], and specify whether it has taken into consideration the total hygrothermal load from outside and inside or not, as it is considered to be less significant for the majority of the current simulation software. However, the interior relative humidity is almost kept manifesting freely without control, while it is difficult to consider the whole heat, air and moisture equilibrium model in order to describe the interrelation between all scales, especially within the building's interior, its envelope and the external climate conditions. Nonetheless, it is important to know that the air pressure gradients within the inside and outside of the building produce air circulation that greatly affect the envelope and building response in terms of heat, air, and moisture transfer. Therefore, compared to outside, moisture buffering has a noticeable influence on indoor water vapor pressure fluctuations [70]. Rain adsorption and moisture residues inside the building envelope may have a significant impact on energy consumption as well as on the performance of the envelope [28]. The indoor relative humidity, if not properly managed, can affect the intended quality of the indoor environment and become a significant potential of poor air quality.

4.1. Nodal approach

The nodal approach is based on the principal that each building zone is a single volume defined as a set of physical variables in uniform states. A node typically represents a room, a floor, or a hall. . . , but it may also reflect something more complex, like internal load such as the heat dissipated by occupancy, equipment, or HVAC system. As a result, one zone is basically equivalent to a node with its own physical parameters, such as temperature, humidity, pressure, etc. For each node of the whole building volume, the heat and

moisture balance equations can be solved using matrix computing methodology.

The nodal approach is a one-dimensional approach that is currently employed in the most common Building Energy Simulation (BES) software, such as TRNSYS, EnergyPlus. Rain adsorption and moisture residues inside the building walls may have a significant impact on energy consumption as well as on the performance of the envelope. Fig. 3 shows a full description of the nodal approach methodology computing for hygrothermal simulation and Table 2 presents a summary of previous studies using the nodal approach.

Coelho et al. [40] took into consideration all the complex geometry in their analysis, such as windows and doors, and regrouped them based on their orientation. They also revealed that using weather files from the same city does not provide the best outputs, and they concluded that the best match was achieved by the weather file of temperature and water-vapor pressure obtained by the monitoring campaign. Their numerical results using the WUFI Plus software were greatly validated by experiments. Furthermore, Moujalled et al. [14] focused, in their work, on a numerical assessment of a building's hygrothermal performance at two scales: wall and envelope. Their key aim was to find more realistic thermal and hygric performance of hemp lime concrete under real climatic conditions. They used the WUFI Pro software as a simulation tool and were able to obtain a good validation of numerical outputs compared to experiments. For extreme cold climates, Wang et al. [71] used a nodal method for their hygrothermal simulations to analyze moisture-safe attic architecture. They reveal that the indoor moisture load levels have a major impact on the hygrothermal conditions of the un-ventilated attic room. As a result, if the indoor moisture level is kept regular and the ceiling air leakage penetration rate is kept below 20%, the moisture-safe conditions in an un-ventilated attic can be reached. In their work, they used WUFI Plus to run their simulation, and the numerical solutions were well validated by experimental.

4.1.1. Strength of the nodal approach

These simulations are based on zone-to-zone continuity equations. They are not only mathematically easier to solve than finite volume/element modeling, but they are also simpler to use because no complex meshing is required. Their computing time is quicker because less calculations are considered necessary. They allow for the evaluation of air flows among zones, air heat balance, humidity and temperature and their variations for each zone, ... According to the literature, four softwares Table 3 are most commonly used for nodal whole-building energy/hygrothermal simulations. They are used to provide physical solutions to a variety

of problems and applications, and all describe the dynamic evolution of indoor relative humidity and temperature as a function of changing outdoor climate and hygrothermal loads, as well as the effect of moisture buffering by indoor condition charges.

Building energy simulation softwares like TRNSYS and Energy-Plus are mainly used to simulate temperature variations and energy demands in specific spaces at a large scale [74]. As a result, moisture exchange models at the wall scale were used in these tools using a simplified model that neglects the coupling of heat and moisture transfer phenomena through the building envelope [75,76].

Currently, there exists other softwares that include Whole Building Heat Air and Moisture (HAM) modeling, e.g. SPARK and WUFI Plus [69,73], which are derived from basic theoretical models of coupled heat and moisture transfers at both wall and envelope scales. These two last-mentioned tools can precisely characterize moisture diffusion and heat transfer within the layers of the building walls, so that the exchange of water vapor between the room air and the outer walls can be accurately described.

4.1.2. Weakness of the nodal approach

In some applications, having a proper understanding of local air conditions and envelope design is critical for assessing local thermal comfort criteria as well as the margin of hygric comfort. For a 1D simplified heat and moisture model for the air volume, this method is not operational. Computational Fluid Dynamics (CFD) can help to obtain a precise prediction of the conditions where a detailed area is needed for heat and moisture transfers in the air or even at the wall scale. Some limitations are listed below:

- The nodal approach has clear weaknesses in investigating some physical evolution, such as temperature, pressure and velocity scalars inside a room.
- It is difficult to perform a detailed analysis of thermal comfort and air quality within a zone.
- The effect of loads on their internal atmosphere is not considered, such as heat dissipation by sun patch [77].
- Temperature distribution according to the length or width of the room is impossible.
- Implementing the nodal approach to a huge room volume (a hall for instance) is very challenging.

4.1.3. Simplified models for simulating surface moisture adsorption and desorption

- Effective Moisture Penetration Depth (EMPD) model

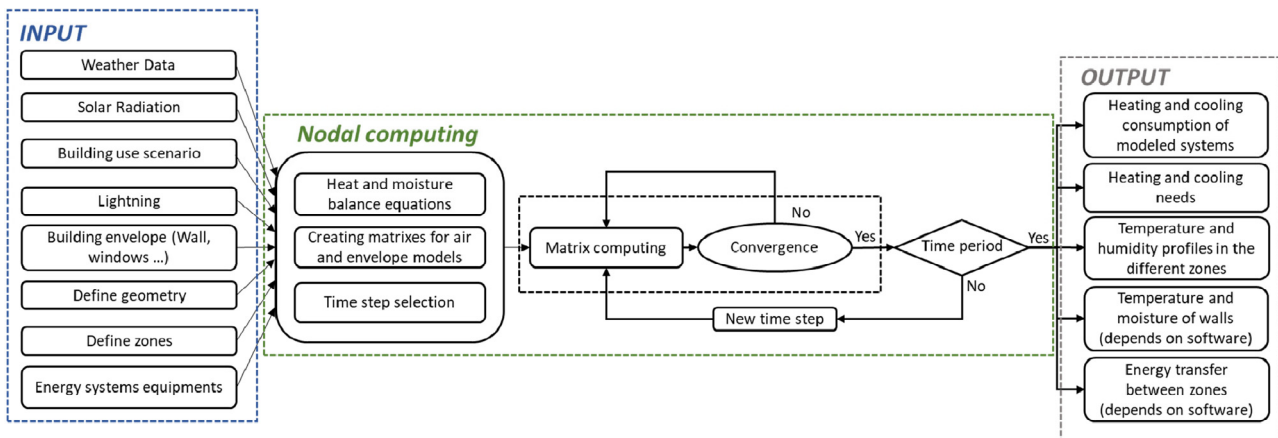


Fig. 3. Detailed schematic description of the Nodal approach for hygrothermal simulation.

Table 2
Summary of building hygrothermal simulation studies based on the Nodal approach.

Study	Nodal Approach	Building scale		Software & models
		Wall	Envelope	
Coelho et al. [40]	✓	x	✓	Wufi Plus. Coupled heat and moisture transfer of Künzel Model. All complex geometry (Windows, doors) were regrouped based on the orientation.
Moujalled et al. [14]	✓	✓	✓	Wufi Pro 5.1 & Matlab. 1D simulation at the wall scale with a coupled heat and moisture transfer inside building walls/Thermography analysis for thermal leaks.
Wang et al. [71]	✓	x	✓	Wufi Plus. Attic zonal model/ Indoor zonal model/Zonal modeling of the HAM building behavior.

Table 3
Summary of the commonly used software for hygrothermal simulation at building scale.

Software	Availability	Model type	HAM model	Numerical scheme	Scale
TRNSYS [26]	Commercial	1D heat and moisture	Simplified (EMPD)	Unsteady state	Envelope
EnergyPlus [72]	Open Source	1D heat and moisture	Simplified (EMPD)	Unsteady state	Envelope
WUFI Plus [73]	Commercial	1D heat and moisture	Full model	Unsteady state	Envelope and Wall
SPARK	Open Source	1D heat and moisture	Full model	Unsteady state	Envelope

The EMPD model simulates surface moisture adsorption and desorption using a simplified mixed solution [78]. Only a thin layer facing the inner or outer surface reacts with the air, known as the sorption-active layer or humidity buffer. This means that water vapor adsorption/desorption between the inside and outside is neglected across walls [11,62], especially those ones that are exposed to external conditions. When exposed to cyclic air humidity fluctuations, the thin layer stores and releases moisture into the room air. Temperature and vapor pressure in that layer are supposed to vary linearly, which is not always the case. Consequently, the thickness of the sorption-active layer is proportional to the effective moisture penetration depth EMPD and the duration of normal vapor pressure variations at the wall surface.

For daily variations, the effective penetration depth for moisture exchange in porous building materials is usually in the order of millimeters. Since moisture adsorption is expressed in this model by a single active sorption layer, only moisture variations with a single cycle, such as daily variations, can be well defined and modeled.

The EMPD method was further developed in the TRNSYS [75] and EnergyPlus [76] codes to address this limit by identifying the moisture buffering as convective mass exchange with the surface layer of the wall and mass diffusion at a deep layer of a few millimeters. Short-term exchanges between the air and the surface buffer, as well as mid-term exchanges using the deeper buffer, can be modeled using this resolution methodology.

• Effective Capacitance Moisture (ECM) model

By assuming that the thermal and humidity parameters in the moisture-buffering layer are the same as in the room air, the previous method of EMPD is simplified even further. As a result, the moisture capacities of the room air, walls, and furniture are merged into a single moisture capacity for the entire room volume [79]. Some building energy simulation softwares use this simplest solution as an effective capacitance moisture model.

4.2. Computed fluid dynamics (CFD) approach

In a nodal approach, the air is considered uniform, while in situations for which low-air circulation regions exist, such as in the area near heating systems, HAM models based on the well-mixed air approximation can provide false results. In fact, the good venti-

lation of wall assemblies can result in higher surface convective transfer coefficients and different transfer potentials than those of hidden partitions [80]. As a consequence, in the HAM transfer approach, only a portion of the wall appears to be engaged for computing, while the rest appears to be effectively inactive. For such scenario, models based on fine spatial discretization of an air volume and accurate conservation equations for mass, momentum, and energy in the air are required.

The simulation of room air using Computational Fluid Dynamics (CFD) approach is necessary for a very accurate study, which allows to calculate with high precision the scalar fields of temperature and vapor pressure in a defined volume. A whole defined volume is usually meshed in a few thousand to a few million control volumes. The conservation equations can be solved using finite element or finite volume methods for each control volume. Solving the Navier-Stokes's equation is one of the basics of software basics that uses the CFD approach (Large Eddy Simulation (LES) or Direct Numerical Simulation (DNS)). It can also solve the mass conservation equation of different species, as well as the conservative energy equation for solid domains and air volumes. As a result, all the governing conservation equations can be expressed:

$$\frac{\partial \phi}{\partial t} + \vec{V}_\phi \cdot \nabla \phi = \Gamma_\phi \nabla^2 \phi + S_\phi \tag{22}$$

Where ϕ stands for many physical parameters like the temperature or the species concentration. Γ_ϕ and S_ϕ are the diffusion coefficient and source term for the standard physical parameter, and V is the velocity vector of ϕ .

ANSYS FLUENT, COMSOL Multiphysics, OpenFoam and other CFD tools are among many choices. They offer a wide variety of numerical solution methods that are not always limited to building energy simulation. Indeed, they can be applied to any system with a detailed simulation plan strategy. Fig. 4 shows a full description of the CFD approach methodology for computing hygrothermal behaviors and Table 4 represents some works on the use of CFD softwares for investigating the hygrothermal transfer at different scales.

Simo-Tagne et al. [81] used a Fortran programming language to simulate the coupled one-dimensional heat and moisture transfer of a wood and concrete wall by applying the finite difference method. The numerical results showed an excellent agreement with the experimental data obtained from the literature for both

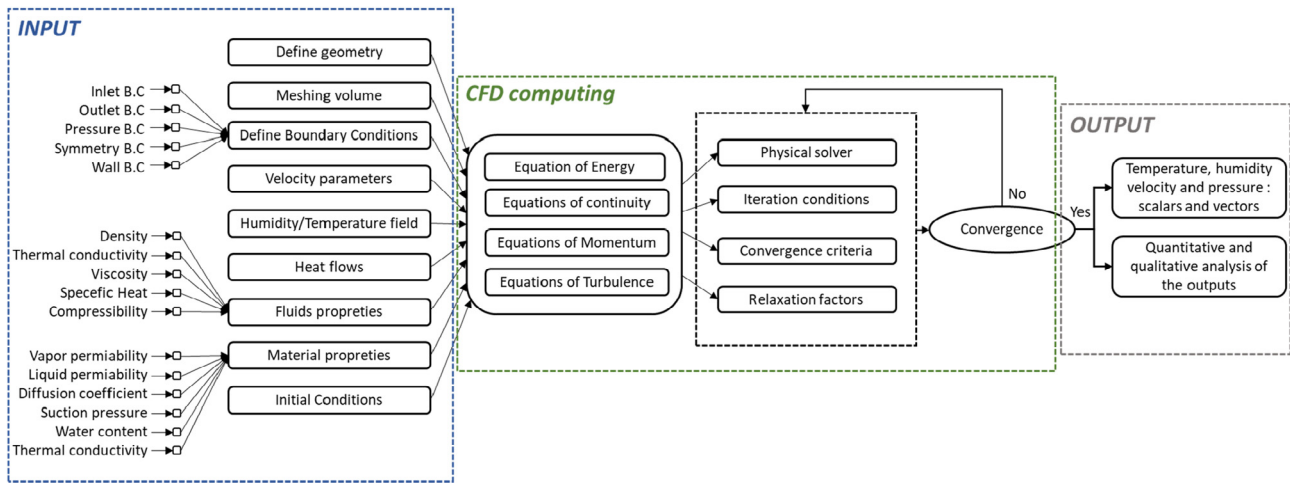


Fig. 4. Detailed schematic description of the CFD approach for hygrothermal simulation.

wood and concrete walls. They also reveal that the lighter wood type is suitable for better insulation of the inside building.

For their simplified one-dimensional numerical model, Alioua et al. [16] used the COMSOL Multiphysics software as the principal simulation tool. The mathematical model of Künzle and Mendes was used to describe the hygrothermal behavior of their Date Palm Concrete (DPC) materials. The authors show that using the hysteresis effect in the models an improvement of the moisture transfer estimation via the DPC wall is operated, and they well validate their numerical simulation outputs with the experimental results. Within the same context, Huang et al. [17] investigated the complex behavior of coupled heat and moisture transfers in their simple one-dimensional model at the wall scale of bamboo laminated panels using COMSOL Multiphysics. They used a climatic chamber to analyze the wall's hygrothermal output experimentally to implement simulation software inputs with material properties. As a result, they showed that the water vapor diffusion resistance factor is the most important factor influencing RH simulation performance while, at steady state, temperature difference is dominated by thermal conductivity. The variance within the relative humidity of the simulation and experimental results is more important than the difference in temperature. Furthermore, according to them, density is the most sensitive parameter, at the transient state, in influencing temperature simulation outputs. However, Seng et al. [12] showed on their model that the moisture diffusion related to the thermal gradient tends to be the primary driving potential of moisture transport when the relative humidity is below 95%. In the other case of a relative humidity above 95%, the enthalpy influence due to the phase transition of water becomes as large as the one of heat transfer by conduction, where the moisture distribution in hemp concrete is mostly driven by liquid transfer at this saturation conditions based on their analysis. For a wall consisting of hemp concrete and rape straw concrete, Promis et al. [15] used also COMSOL Multiphysics software for the 3D modeling of the coupled heat and moisture transfers. For weather inputs, they use the literature data for the climatic conditions. They achieve good experimental validation of the computational simulations results, and show that between 50% and 75% of relative humidity, the hysteresis profile is almost linear.

Hou et al. [39] used a HMCT1.0 software to calculate 1D coupled heat and moisture transfers in multilayer walls made from hollow concrete filled with compressed straw bricks. Their CFD approach is based on a mixed-language programming of FORTRAN and Visual Basic (VB). Thus, to investigate material properties, they rely on a climate chamber with regulated conditions, allowing them to

reveal that the temperature gradient had a significant impact on the diffusion of moisture within the wall. Simulations and experiments were in good agreement. Also simulating a multilayered wall, Labat et al. [60] use the Simulink/Matlab software to simulate the coupled heat and moisture transfer. In this study, the only mechanism considered was vapor diffusion, as the liquid transfer in the porous material being neglected. Their numerical analysis confirms that vapor diffusion had a significant influence on heat flux balance at the building scale, with the latent heat effect being the most important. Several researchers used the FLUENT software for the modeling of heat and moisture transfer such as Van Bellegem et al. [61]. The authors use this software to model heat and moisture transfers in the air and in the porous material at the interface. The authors show that the convective heat transfer coefficient has the largest influence on temperature variations. Additionally, transition of flow type from laminar to turbulent has a low effect on relative humidity within the porous material, because diffusive mass transfer exceeds convective mass transfer. In addition, using the hysteresis model increases the expected relative humidity during the desorption process. They observe also that the heat capacity and thermal conductivity of the porous material had negligible effect on the simulated temperature and relative humidity.

4.2.1. Strength of the CFD approach

For its ability to provide a detailed analysis of the various fluxes that occur inside and outside buildings, the CFD approach is widely used. As a result, it can be considered as an excellent choice for studying the exact variations of the targeted physical parameters on a small scale. In addition, as mentioned above, the volume is meshed into small controlled volumes with uniform or non-uniform meshing, especially near wall-type boundaries to take into account the strong gradients of different physical parameters. This method combines several fundamental principles, such as the equation of mass conservation, momentum and energy equations and the fluid dynamics state equation. It can also include turbulence models if needed, according to the problem of concern. To go further, a coupling of the CFD software with other software interfaces like MATLAB is possible. The CFD approach takes more time to converge to a solution than the nodal approach, but it provides additional information such as detailed airflow scalars and vectors in the zones, as well as air temperature and humidity fields at all points in the space.

Table 4
Summary of building hygrothermal simulation studies based on the CFD approach.

Study	CFD Approach	Building scale			Softwares & features
		Material	Wall	Envelope	
Zhang et al. [34]	✓	✓	x	x	MATLAB. GAB model was considered to fit sorption isotherm curves.
Reuge et al. [35]	✓	x	✓	x	Home-made 1D Cartesian tools for simulation (TMC and TMCKIN). Use of VAN GENUCHTEN model to define the isotherms of adsorption. Thermal conductivities are described by the self-consistent scheme.
Bagaric et al. [36]	✓	x	✓	x	WUFI Pro. Transient numerical simulation. Simulations of energy performance of building according to EN ISO 52016–1:2017.
Dong et al. [37]	✓	x	✓	x	COMSOL Multiphysics & Fortran coding. Hygrothermal behavior is mathematically defined with Künel and Liu model. 1D simulation approach through a porous multilayer wall.
Simo-Tagne et al. [81]	✓	x	✓	x	FORTAN 90 Coupled one-dimensional heat and moisture transfer model. Gauss-Seidel relaxation iteration method is used.
Alioua et al. [16]	✓	x	✓	x	COMSOL Multiphysics. Dynamic coupled heat and moisture transfers. Hysteresis model is considered. A mesh of 50 layers represents a good compromise. Periodic variation of the ambient conditions.
Promis et al. [15]	✓	x	✓	x	COMSOL Multiphysics. Hygrothermal models with the moisture hysteresis effect. Simplify the numerical model (1D approach) GAB model for hysteresis modeling Mass transfer only.
Kang et al. [82]	✓	x	✓	x	Wufi Pro 5.3. 1D simulation at the wall scale. coupled heat and moisture transfer at the wall scale.
Huang et al. [17]	✓	x	✓	x	COMSOL Multiphysics. Dynamic coupled heat and moisture transfer. Simplify the numerical model (1D approach).
Seng et al. [12]	✓	✓	x	x	Programming approach. Implementing the Partial Differential Equations (PDE) in module of FEM package. Complete coupled heat and moisture transfer.
Hou et al. [39]	✓	x	✓	x	HMCT1.0 software. Mixed-language programming of FORTRAN and VB. Coupled heat and moisture transfer for multilayered wall.
Labat et al. [60]	✓	x	✓	x	Simulink/Matlab software. Vapor diffusion is the only mechanism taken into account. The liquid transport in porous media was neglected.
Lelievre et al. [56]	✓	✓	✓	X	COMSOL Multiphysics. Coupled heat and moisture equations model.
Van Belleghem et al. [61]	✓	✓	x	X	CFD Fluent. Heat and moisture transfers in the air, porous material and at the interface is modelled in its full complexity. CFD-HAM coupled models (Solid & fluid domains) Relative humidity is the driving potential.
Qin et al. [83]	✓	x	✓	x	Programming approach. A good agreement is established between the numerical results and the measures values with easy method to determine the material physical properties.

4.2.2. Weakness of the CFD approach

A complete and detailed 2D or 3D modeling of the building with a very fine mesh is required in some cases of study, thus laying bare one of the most important disadvantages of the CFD approach, its high computation time. In fact, the calculation time increases as the mesh size decreases. In addition, the complexity of the model implementation limits the development of the CFD approach. Its use without prior knowledge of fluid dynamics, properties and the solution sets are quite difficult. Furthermore, the prevailing CFD tools, such as ANSYS Fluent [84], OpenFoam [85], and StarCCM+ [86], do not consider coupled heat and mass transfer at the building’s wall scale, with the exception of COMSOL Multiphysics software [87], which has added this option to simulate heat and moisture transport in building materials and at the wall scale (Table 5).

OpenFoam [85] is a CFD software that allows users to access the source code of the physical models and write the desired hygrothermal model (one of those mentioned in the **sub-section**

3.2.4) to model the desired phenomenon. However, this requires a strong knowledge of the C++ programming language.

4.3. Co-simulation of hygrothermal behavior modeling

The main challenge lies in the computation time, and where the time scale is asynchronous is most cases. In nodal approach, it takes a few seconds to perform an annual calculation of the full-scale characteristic of the room’s air for each defined zone. The building envelope, however, requires some hours and sometimes days to achieve the desired results depending on the processor computing capabilities. In this case, for too large calculation times, adopting a coupling softwares strategy might be an issue. Such “co-simulation” methods are typically described as static or dynamic coupling by Zhai et al [88]. The static coupling is the exchange of data between the CFD and the Energy Simulation software in a one- or two-step approach. In fact, the solution’s computation is performed first by one of the softwares, then the

Table 5
Summary of the commonly used CFD software for hygrothermal simulation.

Software	Availability	Model type (simplified)	Numerical scheme	scale	Access to code source
COMSOL Multiphysics [87]	Commercial	heat and moisture model	Steady/Unsteady state	Wall/Envelope	unable
OpenFoam [85]	Open Source	Heat model	Steady/Unsteady state	Wall/Envelope	able
ANSYS Fluent [84]	Commercial	Heat model	Steady/Unsteady state	Wall/Envelope	unable
StarCCM+ [86]	Commercial	Heat model	Steady/Unsteady state	Wall/Envelope	unable

input data is sent to the second program to complete the calculation process with eventually several feedback loops between the two. The dynamic coupling approach, on the other hand, represents a steady exchange of data for each time step during computing. However, this approach is divided into one-time-step dynamic, quasi-dynamic and fully dynamic coupling [89]. Fig. 5 shows the flowchart of the simplified co-simulation methodology and Table 6 represents some works on co-simulations of hygrothermal building behavior.

Berger et al. [9] used MATLAB to investigate the hygrothermal behavior of a wall with different heat and moisture convective coefficient and the Domus Software for the whole-building hygrothermal simulation. In this study, the authors succeed in coupling the two software packages and in reducing the order model in the whole-building hygrothermal simulation. This paves the way for possibility of reducing equations order in the future studies and they showed that the best time step for co-simulation is around 6 min. On the other hand, Zhang et al. [90] used a co-simulation between the 3D CFD STREAM V8 software and the 1D HAM model in porous media. The authors considered the vapor diffusion as the only mechanism acting in moisture transfer, in order to ease the simulation of the coupled hydrothermal model and they considered the relative humidity as the main driving potential.

TRNSYS is one of the software packages used for dynamic thermal simulation of buildings. However, hygrothermal transfer has not yet been implemented in the software, except in few works like the one of as Steeman et al. [62]. The authors used the coupling heat, air and moisture transfer (HAM) in porous materials within the Building Energy Simulation tool TRNSYS with implicit time discretization scheme. The developed coupled model is flexible and is able to simulate multilayered walls with variable boundary conditions in real building application modeling. They rely on analytical solutions and other experimental benchmarks to verify the proper functioning of their co-simulation. Furthermore, several researchers have tested the combination of COMSOL and MATLAB such as Li et al. [91,93]. In their work COMSOL is used to solve the couple heat and moisture partial differential equations, which can operate simultaneously with MATLAB via a graphic user interface. They use the moisture content gradient as the driving potential in their co-simulation, and natural air convection is approached using the Darcy-Boussinesq approximation. Experimental and other numerical benchmarks are used to validate their HAM-BE models.

In previous works, Steeman et al.[92] combined the coupled heat and moisture governing equations of the porous material in FLUENT software through coupling it with the HAM. They used the second upwind scheme for the convective terms and the relative humidity as the primary driving potential of moisture diffusion. When a hysteresis model was used in computational calculations, the results were more consistent with the benchmark data. Finally, their simulations showed that the microclimate vitrine is an excellent protector against relative humidity variations.

4.4. Inputs for hygrothermal simulation tools

All of these methods require some input parameters, such as geometrical data, meshing size, hygrothermal physical variables, meteorological data, equipment loads, and comfort scenario. These parameters, on the other hand, are always expressed with some complexity. There are also uncertainties caused by the simplifying hypotheses in addition to the different parameter's estimation error. Therefore, to reduce the sophistication of the hygrothermal dynamics evolution that exist in buildings, some assumptions with implications for model efficiency must be made. Due to all these difficulties, it is extremely difficult to understand the degree of precision of the model. As a result, it seems challenging to put together the heat and moisture transfers phenomenon of a building into a general overview without accumulating too many complex technics. In the following we poke for the main parameters that influence simulations.

4.4.1. Geometry

Before any hygrothermal analysis, whether using the CFD or the Nodal approaches, the enclosure geometry must be well defined. Or when using a calculation program like FORTRAN, it does not require a graphical interface to model the geometry [37,81,83]. However, the enclosure geometry for the CFD or Nodal approach must provide macro building data, enclosure assembly details and micro-details.

4.4.2. Mesh generation

The meshing process is important for the quality of the simulations, and it is only necessary for the CFD approach. The nodal approach does not require any meshing because each zone or building volume is assigned to a single global mesh. The procedure of dividing the studied zone into small elementary volumes is

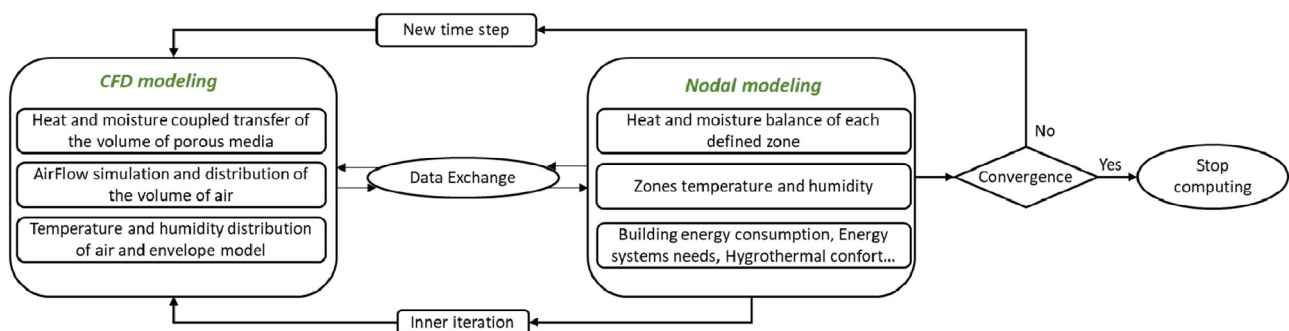


Fig. 5. Co-simulation simplified flowchart.

Table 6
Summary of co-simulation studies on hygrothermal behavior of buildings.

Study	Building scale			Coupled softwares	CFD approach	Nodal approach	Multilayered wall
	Material	Wall	Envelope				
Berger et al. [9]	x	✓	✓	Matlab (Wall) Domus (Building)	✓	✓	x
Zhang et al. [90]	x	✓	✓	CFD STREAM V8	✓	✓	✓
Steehan et al. [62]	x	✓	✓	TRNSYS HAM tool	✓	✓	✓
Li et al. [91]	x	✓	x	COSMOL Multiphysics MATLAB	✓	✓	✓
Steehan et al. [92]	x	✓	x	FLUENT HAM model	✓ Heat in solid/HAM in fluid/EPD model	✓	x

known as the mesh pre-processing step for any numerical study. Meshes should be fine in areas where velocity, temperature or pressure gradients are the most highly significant. If these areas cannot be anticipated, it is suggested that iterative mesh size modification checks should be performed to study their sensitivity in regard to the output of the final numerical results as already done by Alioua et al. [16]. In the case of wall heat and moisture transfer analysis, the simulation softwares recommend particular ways to mesh the boundary layer near the wall so that the coefficients and physical phenomena at this region can be calculated more efficiently and precisely. A sensitivity analysis of the mesh is necessary in most numerical modeling and especially for the CFD approach. This requires performing, at each time, simulations with a higher number of meshes. If the results of the simulation depend on the mesh, it is advisable to refine the mesh until obtaining an independence between outputs and mesh sizes. This means that the results are no longer dependent on the grid resolution. We must know that any local events, such as air recirculation, flow clogging, hot areas and etc . . . , would not be caught if the mesh size is too large. It is worth noting that Steeman et al. [62] based their study on a mesh thickness that varies from 3 mm to 7.7 mm, while Skerget et al. [94] used 200 layers for 1D discretization mesh of a wall thickness equal to 36.5 cm and Alioua et al. [16] used 100 meshing layers for a wall thickness of 15 cm.

4.4.3. Material properties

When employing a CFD or Nodal methods to simulate the hygrothermal behavior of buildings, a large number of material properties is needed. For instance, Specific heat, thermal conductivity, hygroscopic material’s water vapor permeability, apparent density, water absorption coefficient, sorption isotherm, and hydraulic conductivity are typical material properties required as a primordial input for hygrothermal simulation. The values of the previous parameters can be altered by temperature, humidity and moisture content. In fact, they can change proportionally because of these factors or vice versa. When simulating the hygrothermal behavior of a hygroscopic wall on COMSOL Multiphysics [87], for example, such material properties for moisture transport are demanded, as water content, liquid and vapor permeability, diffusion coefficient, and suction pressure, as well as thermal properties such as, thermal conductivity and specific heat [95].

Two phenomena observed in hygroscopic materials are important for the accuracy of the simulation: (i) Sorption isotherm and (ii) Hysteresis effect. The models describing these two phenomena are presented below:

4.4.3.1. Sorption isotherm

At constant atmospheric conditions except for humidity, the water sorption isotherm represents the thermodynamic relationship between water movement and the equilibrium moisture content of a hygroscopic material. Adsorption and desorption are two quite different processes, which describe the equilibrium water

content as a function of atmospheric relative humidity at a specific temperature (Fig. 6). Consequently, isotherms can be considered as one of the most important moisture diffusion properties of porous building materials. Then, sorption isotherms can be generated either from an adsorption process or from a desorption process.

The evolution of phase change heat is often followed by the adsorption and desorption of a gas on porous surface. It is determined by the interactions between the adsorbent and the adsorbate. The heat is released to the atmosphere during adsorption and captured into the system during desorption.

A variety of mathematical models have been developed to account for sorption isotherms, including linearity or non-linearity models with partial coefficients as parameters. A model well suited for one kind of hygroscopic material is not always suitable for another, and the model only has a suitable predictive value for a limited range of moisture activity. Moisture sorption isotherms can be defined using semi-empirical equations with two or three suitable parameters. The GAB formula and the BET equations are the most widely used to describe sorption isotherms in construction materials, but others like the Langmuir, Van Genuchten . . . have been also used. The Clausius-Clapeyron equation were used in several studies [11,13] to describe the sorption curves as a function of temperature.

- Brunauer, Emmett, and Teller (BET) Model

Brunauer, Emmett, and Teller suggested the BET model, which became the most commonly used model to describe sorption curves in hygroscopic media [59]. It is a fundamental principle in the understanding of multilayer sorption isotherms, and its model can be written as follow:

$$w = \frac{X_0 c \phi}{(1 - \phi)(1 - \phi + c\phi)} \tag{23}$$

Where X_0 is the monolayer moisture content, which is the point at which the water is connected to every ionic group, c is the energy constant for the specific heat of sorption, which represent the difference of energy sorption by the molecules of the first layer and the molecules of remaining layers, and ϕ is the relative humidity.

- Guggenheim-Anderson-de Boer (GAB) model

Guggenheim [96], Anderson [97], and De Boer [98], individually developed the equation of this model in 1966, 1946, and 1953, respectively. The GAB model is a refinement of the Langmuir [99] and BET models of physical adsorption, and contains several benefits over the others, by including a valid theoretical framework. According to this model, the adsorbed molecules in the second layer are in the same state as those in the superior layers deposited later, but different from those in the liquid state. These authors proposed a second sorption process for the classified adsorber molecules. The standard chemical potential difference

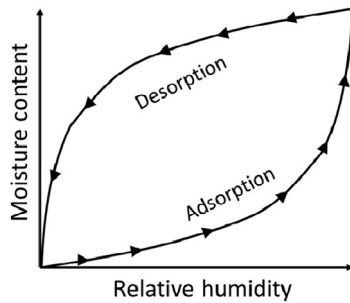


Fig. 6. Humidity sorption isotherm as a function of relative humidity.

between the molecules in this second coat and those in the pure liquid state is represented by a third constant, defined as k , for the any isotherm evolution based on the GAB model. Hence, the current model is expressed as:

$$w = \frac{X_0 c_g k \varphi}{(1 - k_g \varphi)(1 - k_g \varphi + k_g c \varphi)} \quad (24)$$

Where X_0 is the monolayer moisture content, c_g and K_g are the adsorption constants, which are proportional to the energies of interaction between the first and eventual adsorbed molecules at each sorption level. Therefore, they can be expressed theoretically as it indicated in the following equation:

$$c = c_0 e^{\left(\frac{H_0 - H_n}{RT}\right)} \quad (26)$$

$$k = k_0 e^{\left(\frac{H_n - H_l}{RT}\right)} \quad (27)$$

Where H_0 , H_n , and H_l are the molar sorption enthalpies of the monolayer, followed-layer on top of the monolayer, and the bulk liquid, respectively. Also, c_0 and k_0 are the entropic adjustment factors. T is the absolute temperature, and R is the ideal gas constant. It is worth noting that The GAB model transforms into the BET equation when K is equal to 1.

The GAB model is often considered as a suitable approach to model isothermal sorption curves thanks to the explicit thermodynamic state functions taken into account. It is consequently able to explain sorption activity in a wide range of likely values between 0% and 90%. For relative humidity values above 93%, the GAB model underestimates the moisture content values, especially when there is a lot of moisture activity in liquid form. This model has been used in many studies [12,15,16,34,56] for the approximation of sorption isotherms.

• Van Genuchten model

The Van Genuchten model [100] is simple and commonly used in fitting measured isothermal sorption curves of hygroscopic materials [14,35,91]:

$$\theta = \theta_r + \frac{(\theta_s - \theta_r)}{(1 + (\alpha \cdot h)^n)^m} \quad (28)$$

With $m = 1 - (1/n)$ and n greater than 1

Where θ is the moisture content, θ_s is the saturated moisture content, θ_r is the residual moisture content, h is the capillary pressure, and α , m and n are the optimization parameters.

4.4.3.2. Hysteresis effect

Hysteresis of water vapor sorption isotherms has long been identified as one of the most important factors affecting moisture transfer within building materials. Sorption curves represent the main adsorption and desorption evolution lines. Sorption hysteresis is a phenomenon that happens as sorption isotherms shift from

the main path when drying and wetting operations occur (Fig. 7). Several studies have found the existence of hysteresis effect between desorption and adsorption nearly through the entire relative humidity range.

For the simulation of moisture transfer in adsorption and desorption cycles, some models ignore the hysteresis effect and use the main sorption isotherm. Although, numerical simulations that consider hysteresis have recently become a subject of common interest to ameliorate numerical results such as Moujalled et al. [14] study. The authors used a real building envelope to investigate experimentally and numerically the hygrothermal behavior of the building. In their co-simulation work showing a good agreement between simulations and experiments, the hysteresis is modelled in MATLAB since WUFI cannot take it into account.

The impact of the sorption hysteresis phenomenon on heat and moisture transfer in expanded polystyrene concrete was studied by Maaroufi et al.[101]. They integrated the hysteresis model in MATLAB and coupled it to COMSOL Multiphysics, where the coupled heat and moisture transfer model was applied to account for the hysteresis effect of adsorption and desorption. Their coupled model leads to a better understanding of hygrothermal behavior while minimizing the difference between the numerical and experimental results from 28% to less than 7%. Hereafter some models describing sorption hysteresis cycles are presented.

• Mualem II model

Mualem II model [102] allows the prediction of the scanning curves from two boundary curves. The primary drying scanning curve starts at a suction ψ_1 on the boundary wetting curve and can be calculated as:

$$\theta(\psi_{\min}, \psi_1, \psi) = \theta_w(\psi) + \frac{[\theta_w(\psi_1) - \theta_w(\psi)]}{[\theta_u - \theta_w(\psi)]} [\theta_d(\psi) - \theta_w(\psi)] \quad (29)$$

Where $\theta_w(\psi)$ and $\theta_d(\psi)$ are the water contents on the boundary of wetting and drying curves at suction respectively, and θ_u is the water content at the meeting point of the two boundary curves. The primary wetting scanning curve is given by:

$$\theta(\psi_{\max}, \psi_1, \psi) = \theta_w(\psi) + \frac{[\theta_u - \theta_w(\psi)]}{[\theta_u - \theta_w(\psi_1)]} [\theta_d(\psi_1) - \theta_w(\psi_1)] \quad (30)$$

So, the wetting after a series of alternating processes of drainage and adsorption is written as following:

$$\begin{aligned} &\theta(\psi_{\min}, \psi_1, \psi_2, \dots, \psi_N, \psi) \\ &= \theta_w(\psi) + \frac{[\theta_d(\psi_N) - \theta_w(\psi_N)]}{[\theta_u - \theta_w(\psi_N)]} \cdot [\theta_w(\psi_{N-1}) - \theta_w(\psi)] \\ &+ \sum_{i=1}^{(N/2)-1} \frac{[\theta_d(\psi_{2i}) - \theta_w(\psi_{2i})]}{[\theta_u - \theta_w(\psi_{2i})]} \cdot [\theta_w(\psi_{2i-1}) - \theta_w(\psi_{2i+1})] \end{aligned} \quad (31)$$

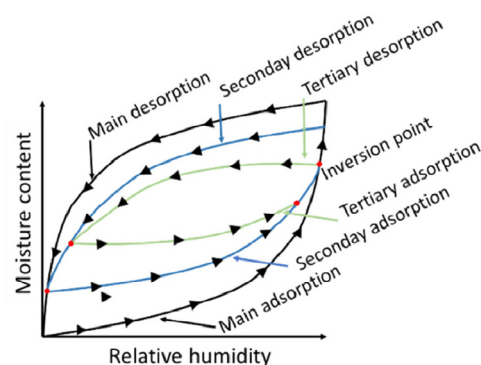


Fig. 7. Schematic representation of the intermediate variations of the hysteresis phenomenon of the sorption curves.

And the drainage after a series of alternating processes of drainage and adsorption:

$$\begin{aligned} &\theta(\psi_{\min}, \psi_1, \psi_2, \dots, \psi_N, \psi) \\ &= \theta_w(\psi) + \frac{[\theta_d(\psi) - \theta_w(\psi)]}{[\theta_u - \theta_w(\psi)]} \cdot [\theta_w(\psi_N) - \theta_w(\psi)] \\ &+ \sum_{i=1}^{(N-1)/2} \frac{[\theta_d(\psi_{2i}) - \theta_w(\psi_{2i})]}{[\theta_u - \theta_w(\psi_{2i})]} \cdot [\theta_w(\psi_{2i-1}) - \theta_w(\psi_{2i+1})] \end{aligned} \quad (32)$$

This model has been used in many studies [15,16,56,61,92] to take into account the hysteresis effect in sorption cycles of adsorption and desorption of hygroscopic construction materials.

• Pedersen Model:

Pedersen [103] assumes that depending on the complexity of the movement of the water content context in the material, the intermediate curves shift asymptotically towards the main adsorption or desorption curves. The principal adsorption and desorption curves, as well as the primary adsorption and desorption loops, must be determined experimentally in Pedersen’s model.

Knowing the water capacities for the main curves, the analytical representation of the water capacities of the intermediate adsorption/desorption curves can be expressed:

$$u_{new} < u_{old} : \xi_{hys} = \frac{(u - u_a)^2 \xi_d + 0.1(u - u_d)^2 \xi_a}{(u_d - u_a)^2} \quad (33)$$

$$u_{new} > u_{old} : \xi_{hys} = \frac{0.1(u - u_a)^2 \xi_d + (u - u_d)^2 \xi_a}{(u_d - u_a)^2} \quad (34)$$

Where ξ_{hys} is the moisture capacity at hysteresis, ξ_a is the adsorption moisture capacity at the current RH, ξ_d is the desorption moisture at the current RH, u is the current moisture content, u_a is the adsorption moisture content corresponding to current RH-Value, and u_d is the desorption moisture content corresponding to current RH-Value.

• Huang’s hysteresis model

Based on the Kool and Parker model [104], Huang et al. [105] introduced a new hysteresis model to characterize intermediate sorption curves in soils. After a sequence of alternating sorption cycles, the adsorption and desorption curves can be written [106]:

$$Adsorption : u(RH, i) = u_r(i) + (u_s(i) - u_r(i)) \frac{u_{ads}(RH)}{u_{sat}} \quad (35)$$

$$Desorption : u(RH, i) = u_r(i) + (u_s(i) - u_r(i)) \frac{u_{des}(RH)}{u_{sat}} \quad (36)$$

Where $u_r(i)$ and $u_s(i)$ are the residual and saturated moisture contents of the scanning curves respectively, u_{ads} and u_{des} are the main curves for adsorption and desorption.

4.4.4. Boundary and initial conditions

In addition to the physical modeling of heat and moisture transfer coupled equations, boundary conditions are often essential for the output’s quality of the numerical resolution of the mathematical models.

For both nodal and CFD approaches, the following aspects must be known, as the interior climate, exterior environment, and boundary conditions between components. The proper pre-processing of interfacial interactions at the boundaries between control volumes (fluid or solid domain), is crucial for an effective modeling. The following models are presented to describe the exterior environment and interior environment, heat balance on

outdoor and indoor wall surfaces, and vapor balance on inside and outside wall interfaces.

• Exterior environment

For most HAM models, the outside ambient air or exterior atmosphere is generally determined in terms of hourly meteorological parameters. The temperature and relative humidity of the outdoor air, solar radiation incident on the ground, and rain load incident on the external wall are the climate data that most hygrothermal softwares need on an hourly basis. Furthermore, wind velocity and direction are common climatic data that are required for hygrothermal simulations. All of the above data may be measured with a weather station [14], estimated with weather software instruments, or extracted from a quantitative treatment of meteorological datasets [38,40,60,71,91]. However, for the CFD approach, it is difficult to describe climatic conditions such as rain load without using other physical model equations, which can increase computation time. Consequently most of the research works include an imposed climatic condition in form of equations [11,14,34,94]. The CFD method offers simple calculation for wind scenario such as speed and orientation, with a computation time step Δt much smaller than the nodal approach, ranging usually from few seconds to few minutes, but usually less than 5–6 min [9].

• Interior environment

The dynamic values of temperature and relative humidity define the indoor ambient climate, also known as the interior environment. There exist a few standards for indoor climate rule simulation (Iso, ASHRAE...) to assess thermal comfort indexes. Thermal comfort indexes allow the evaluation of an energy balance of the building. The hygrothermal balance of the building envelope is presented below.

• Outside Surface Heat Balance

The balance is expressed by the following equation:

$$-\lambda \frac{\partial T}{\partial X} \Big|_{ext} = h_{c,ext} \cdot (T_{air,ext} - T_{surface,ext}) + Q_{rad,sky} + j_v \cdot L_v \quad (37)$$

Where $h_{c,ext}$ is the convective heat exchange coefficient of the exterior face, j_v is the mass flow density of moisture vapor diffusion and L_v is the latent heat of evaporation. The convective and radiative heat transfers with the ambient air are described by the first two terms of the right-hand side. The third term deals with the specific enthalpy of the energy carried by the water vapor, in which only the latent part is taken into account, while the sensible part is neglected. Therefore, for the sensible specific enthalpy, the reference temperature is defined as zero.

• Vapor and capillary balance on outdoor wall surface

The balance is expressed by the following equation:

$$-\delta_p \frac{\partial P}{\partial X} \Big|_{ext} = \beta_{v,ext} \cdot (P_{vap,air,ext} - P_{vap,surface,ext}) \quad (38)$$

The convective moisture transfer with the ambient air is represented by the term on the right-hand side. In this equation δ_p signifies the water vapor permeability and β_v indicates the convective mass transfer coefficient, which is dependent on the air velocity near the surface.

It can often be assumed that there is no liquid flux at the indoor boundary surface for the wet surface state on the vertical

wall. If there is no wind-driven rain, the assumption is also true for the outer boundary surface. Otherwise, on the exterior wall, rain can cover the surface, which eventually becomes saturated. There are two possibilities: When the incident rain is not enough to saturate the outer wall layer and when all of the available moisture is adsorbed into the wall:

$$m_w = k_w \frac{\partial P}{\partial Z} \tag{40}$$

The capillary transfer rate limit is surpassed by the incident rain on the wall layer on the outermost wall layer, and the moisture excess is drained from the surface:

$$m_{rain} = k_w \frac{\partial P}{\partial Z} \tag{41}$$

Where m_w is the mass flux for liquid water and m_{rain} is the mass flux for rain and K_w is the liquid water permeability.

• Inside Surface Heat Balance

This balance is expressed using the same boundary conditions as for the external surface except for the radiative exchange which comes from internal sources that emit radiation:

$$-\lambda \frac{\partial T}{\partial X} \Big|_{int} = h_{c,int} \cdot (T_{air,int} - T_{surface,int}) + Q_{rad,int} + j_v \cdot L_v \tag{42}$$

Here the convective and radiative heat exchanges with the ambient air are described by the first two terms on the right-hand side of Equation (42). The third term defines the enthalpy of water vapor transfer through the building envelope.

$$Q_{rad,int} = \frac{W_r}{\sum_i A_i} + h_{r,int} (T_{surrounding} - T_i) \tag{43}$$

Where W_r represents the total of all radiative heat sources in the volume area. The radiative heat transfer from the surrounding surfaces is presented in the second term, in which $T_{surrounding}$ represents the average surface temperature of all surfaces in an area. The part that passes through a transparent medium, such as a window, is counted as a heat loss in this case. T_i is the indoor air temperature.

• Vapor balance on indoor wall surface

The balance is expressed by the following equation:

$$-\delta_p \frac{\partial P}{\partial X} \Big|_{int} = \beta_{v,int} \cdot (P_{vap,air,int} - P_{vap,surface,int}) \tag{44}$$

Here the same basics applied to boundary conditions on the outdoor surface stand, with the exception that this one interacts with the indoor air, and the moisture convective transfer coefficient can be correlated to the heat convection coefficient of the indoor environment in some cases.

Taking into account sorption and hysteresis models, the type of boundary conditions used, the various components potentially used in the calculations . . . , a thorough examination of the literature (Table 7) indicates that no work carried out so far addressed the case of hygrothermal bridges.

• Discussion on the physical models

Several physical methods for building energy simulation were listed in the preceding sections. We saw in the previous examples that the concepts of each technique and each physical approach has its own application domain. The CFD is the most accurate and descriptive technique. It allows for a detailed description of each mechanism in the building envelope. It is particularly well

Table 7 synthesis of parameters and application models for hygrothermal behavior simulation of porous media.

Study	Hygrothermal bridges	Sorption model	Hysteresis Model	Calculation method	Numerical Dimensions	EMPD Model	Solar Radiation	Heat and moisture convection	Experimental validation	Boundary conditions type
Zhang et al. [34]	x	GAB	x	Programming on MATLAB Künzel model	2D & 3D	x	x	x	✓	Dirichlet
Reuge et al. [35]	x	Van Genuchten	x	Not indicated	1D	x	x	✓	✓	Neumann
Alfoua et al. [16]	x	GAB	Muallem II	Finite element	1D	x	Defined as radiation coefficient	✓	✓	Neumann
Promis et al. [15]	x	GAB	Muallem II	Finite element	3D	x	x	✓	✓	Neumann
Moujalled et al. [14]	x	Van Genuchten	Huang	Finite difference	1D	x	✓	✓	✓	Neumann
Colinart et al. [13]	x	Clausius-Clapeyron equation	x	x	1D	x	✓	✓	✓	Neumann
Seng et al. [12]	x	GAB model	x	Finite element	1D	x	x	✓	✓	Neumann and Dirichlet
Lelievre et al. [56]	x	GAB	Pedersen and Muallem II	Finite element	1D	x	✓	✓	✓	Neumann
Van Belleghem et al. [61]	x	✓	Muallem II	Finite volume	2D	x	x	✓	✓	Dirichlet and Neumann

suitable to modeling the convective exchange that occurs in a broad zone volume.

However, due mainly to the long calculation times, it is hard to model all physical phenomena using CFD. Accordingly, it is necessary to use it in combination with the nodal approach as implemented in EnergyPlus or TRNSYS. The nodal modeling is well suited to consider global resolution as uniform field parameters, compared to the CFD simulation, where the physical phenomenon is represented in a less detailed form. When a physical simplification is theoretically feasible, the objectives become to simplify the principal computational model of the solving processes by linearizing the maximum number of physical equations as possible. Table 8 summarizes the difference between the two most commonly used approaches to simulate the building behavior in the current scheme that have been used and validated in previous research.

The inputs of material properties and the boundary conditions needed for hygrothermal modeling have been identified in section 4.4. Since the aim of most hygrothermal models is to include enough and accurate details for a well and smooth simulation running, we have put a list of suggestion to follow when modeling a single part of the building envelope or a multizone structure.

The software's efficiency in evaluating a given single component or multi-zone building hygrothermal behavior should ideally be based on previous works' reliability and on their validation by benchmarks. If this is not possible, it is preferred to choose the tool based on the software's numerical modeling solvers and inputs. Since the diverse softwares have various hygrothermal features, strengths and limitations like the capability to model heat and moisture transfers by air or diffusion through envelopes in, 1D, 2D, or 3D scale, or the ability to simulate a large number of zones in a reasonable amount of time, future investigators would need to choose hygrothermal simulation methods that are ideally matching their goals:

- Accurately estimating and validating results.
- Allowing effective data input and verification.
- Knowledge of all the inputs needed for the simulation.
- Being adaptable to solving non-standard problem types.
- Providing quick output post-processing.

5. Statistical methods using machine learning

Artificial intelligence is a branch of computer science that focuses on machine learning. Also known as a data-analysis-based computing approach. Although AI refers to a collection of sophisticated mathematical and processing approaches that allow

Table 8
Main difference between CFD and Nodal approach.

Nodal approach	CFD approach
Flow between zones, outputs, inputs Heat balances, thermal deprecations (Including thermal bridges, under crawl space...)	Detailed modeling of air flow and its parameters within zones More efficient modeling of the physics phenomenon within the solid and volume domains
Energy balance equations	Reynolds Average Navier Stokes Equations Large Eddy Simulation Direct Numerical Simulation
Less complex resolution method, faster calculations node = 1 zone = 1 Mesh	Detailed calculations requiring a longer resolution time Meshing a whole volume into few thousands to few millions of small elements or volumes
Climate data, includes temperature, relative humidity, solar radiation, rain load and etc.	Describing climatic conditions such as rain load needs the use of other physical model equations.

models to learn from the data they collect and use that knowledge to perform a variety of critical aspects. This section presents the Artificial Neural Networks (ANN), a type of artificial intelligence. It provides all we need to know about neural networks, including layers, neurons, connections, weights, and activation functions. It also goes through the modeling rules for an ANN architect. The following subsections explain how ANN are developed and illustrate all the details of neuron network processing.

5.1. Artificial neural networks modeling

Artificial neural networks have been commonly used in a variety of fields thanks to their ability to solve complex issues by learning directly from input data. A neural network is a data processing model inspired by the human brain's ability to learn from observations and interpret by abstraction.

An ANN is a highly parallel distributed processor made up of basic processing units with a natural tendency for encoding experimental data and making them available for analysis use. Because of its robustness in solving quantitative and nonlinear simulation problems, such as function estimations and identifications, ANN is often used as a proxy model or as an approach based on a response surface approximation.

The architecture of ANN consists of a number of inputs, outputs, hidden neurons, a number of hidden layers. However, this does not indicate that an ANN with a single hidden layer is the best choice in terms of robustness, learning time, and application. In fact, there is actually no standard rule for determining the best ANN architecture for a given set of input and output data.

5.2. Artificial neural networks principles

For general energy problems [107,108], ANNs are undoubtedly among the main soft-computing approaches. There is a number of logical explanations for this. First and foremost, it has the potential to correctly understand the basic interaction of any range of input and output data without the use of a physical model.

This approach's capacity is not largely influenced by the underlying relationship's complexities, including non-linearity, various variables and conditions, external perturbation, and ambiguous input and output data. As a consequence of learning technics for the ANN building architect, this vital skill is known as pattern recognition.

In addition, due to the large number of processing units in the network that perform extensive parallel processing of data, the methodology is designed to be fault tolerant. Also, the methodology's learning capacity allows it to respond to changes in the parameters. Via neuro-controllers, the ANN can handle time-dependent apprenticed and dynamic simulation.

This capability allows energy engineering to dive into the predictive model analysis and parameters, at a high level of sophistication, that can hardly be handled by the conventional physical analysis at the moment, such as the nonlinearity of heat and moisture convective transfer at boundary layers.

5.3. Artificial neural networks architectures

Layers of neurons are used to build an Artificial Neural Network. The input layer is the first layer of neurons, X_i (Fig. 8), receiving the input signals x_i for the generation of the input from the outside environment. The output and last layer of neurons, Y_j , are generating the network's output of signals y_j .

Between the input and output layers are located hidden layers of neurons which are used to execute the majority of the calculations. Between each layer and the following one, associations are operated through artificial connections.

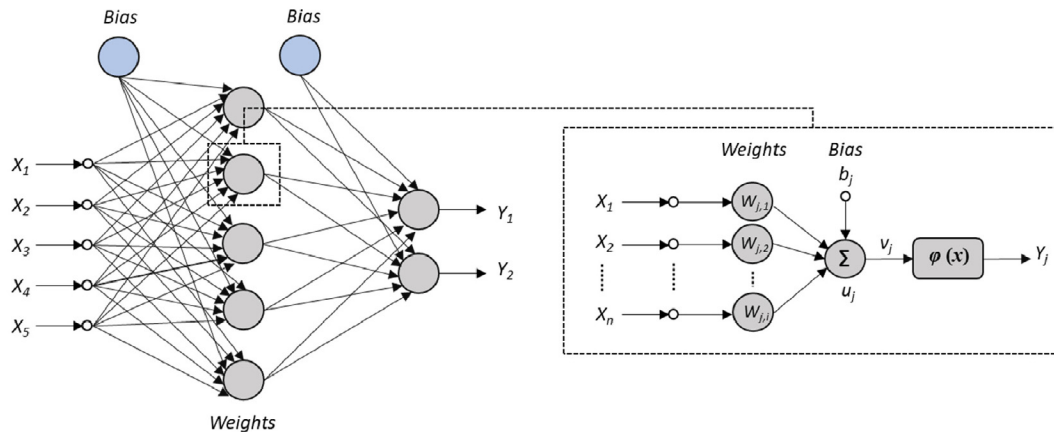


Fig. 8. Feed-Forward of Artificial Neural Network architect with a nonlinear model of a neuron.

ANN can be classified into two groups based on their association pattern [109], recurrent (feedback) networks or feed-forward networks. A feed-forward network is, in the sense that it generates exactly one set of output values from a given input. The most common class of feed-forward networks has unidirectional relationships between layers. These networks are characterized by being memoryless in the sense that their reaction to an input is unaffected by the network’s previous condition. A recurrent or feedback networks is a dynamic system. The neuron outputs are calculated when a new input pattern is introduced. The inputs to each neuron are then changed as a result of the feedback paths, causing the network to reach a new state.

• Weights

Each neuron in the previous layer is linked to a neuron in the layer after it, which gives to the connection a weight assigned to it, and each weight has two indexes. The receiving neuron number defines the first index of the weight, and the submitting neuron number is the second index. The weight is applied to the relation between the second hidden layer neuron and the only input layer neuron.

• Bias

Since any input information can be somehow biased, such a bias, u_j , is potentially attributed to each neuron layer (Eq 45) Biases enable the linear part of each neuron’s output measurement to follow the approximated function architecture more easily.

The neuron model can be described using the following mathematical expressions:

$$u_j = \sum_{i=1}^n w_{ij}x_i + b_j = v_j + b_j \tag{45}$$

where x_1, x_2, \dots, x_n are the input signals; $w_{1j}, w_{2j}, \dots, w_{ij}$ are the respective synaptic weights of the neuron j , b_j is the bias weight at layer level j , u_j is the linear combiner output due the input signals, $\varphi(\dots)$ is the activation function, v_j is the induced local field and y_j is the output signal of the neuron.

• Activation function $\varphi(x)$:

In order to define the output state of each neuron, either active (“on” or “1”) or inactive (“off” or “0”), a nonlinear activation function of the inputs is used. For ANN, a variety of activation functions have been used. Their utility is determined by various parameters

like the interval in which they behave without too quick saturation, the speed at which the function varies as its argument changes, as well as the main interests in their computing [110].

One of the most widely used activation function is the threshold function, also known as Heaviside function (Fig. 9). Using such a function, the output of the neuron is 0 if the input of that neuron is negative, and 1 otherwise. Another often used function is the logistic sigmoid, the abruptness of its transition between the two asymptotic values being adjustable by the variation of δ . The hyperbolic tangent function is also used as an activation function, but this latter does not allow the modification of the transition abruptness.

For this reason, the input data to the network are usually normalized on a specified interval because certain activation functions perform well on a defined interval and the input data are also normalized on that interval. Therefore, various studies use activation functions such as the threshold function, the logistic sigmoid function, the hyperbolic tangent, the Gaussian, and others. From one hidden layer to another, the activation function may be replaced. The logistic sigmoid function, which has continuous derivatives to overcome computational difficulties, is the most preferred and commonly used activation function.

5.3.1. Learning methods in ANN

From a range of combined data, ANN can learn complex relationships between inputs and outputs. Preparing data for pre-processing analysis and before network teaching is a crucial step in making ANN functions effective and due to the obvious significant variance between data input and neural network output, data scaling can be used in this case.

The connection weights are usually identified by the artificial neural network from available training data. Where, the iterative updating of the weights in the network improves performance over time, and ANNs’ ability to benefit as much as possible from provided data makes this methodology very interesting.

ANNs tend to learn core concept rules, such as input-output relationships, from a sorted number of representative instances, rather than following a series of rules defined by a specified case of studies. As a result, this statistical modeling is more reliable than the traditional physical modeling in some cases.

The network’s learning rate is crucial in limiting the amount of adjustment made to the weights and biases. However, in some cases, oscillatory error behaviors will prevent the ANN from reaching the desired outcome. Typically, 70 to 80 percent of the teaching data is used to train the network, while the rest is used to verify the network’s accuracy. We need to know the ways in which the net-

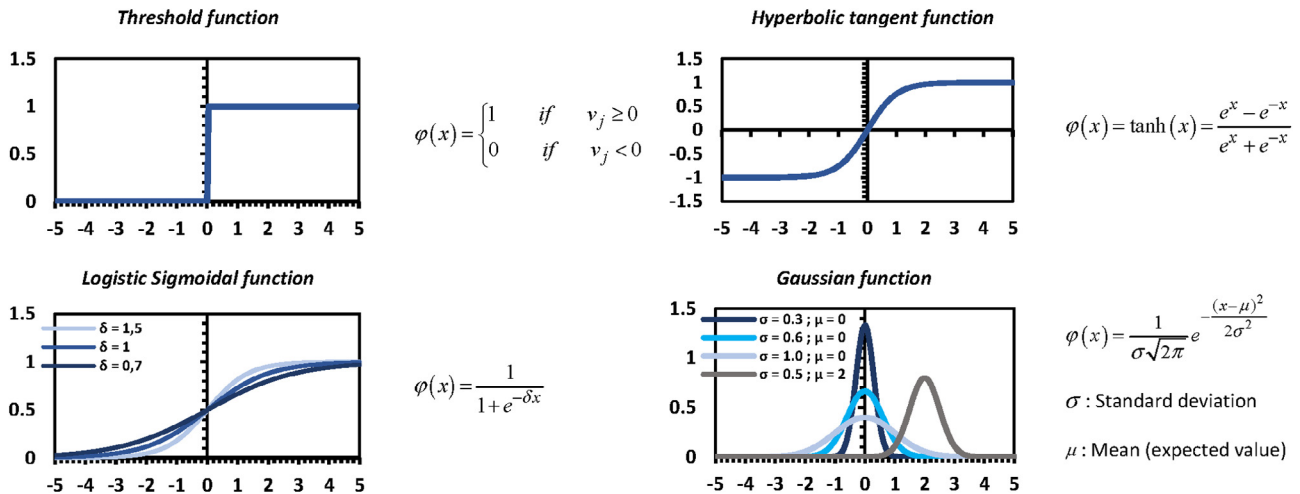


Fig. 9. Different activation functions of a neuron.

work weights are changed with the aim of determining the updating process, in which a learning algorithm which refers to the desired procedure can be used to adjust the weights based on the needs (Fig. 10).

Learning with a teacher (supervised learning) and learning without a teacher (unsupervised, and reinforced learning) are the two primary learning concepts [111]. In learning with a teacher (supervised learning) and for each input data, the network is given a valid response of output data which gives the network's weights the ability to generate results that are similar to the known validated answers.

In reinforcement learning, which is a type of learning without a teacher, the network is given only critical conditions on the validity of network outputs, not the right answers themselves to produce the right architecture of the ANN model. In unsupervised learning, on the other hand or learning without a teacher, would not necessitate a right response for input data in the training procedure. It investigates the fundamental basis of the data, or associations between variables, gathers structures into categories based on similarities and allows researchers to use a competitive-learning method to do unsupervised learning on occasion. As we can illustrate a neural network with two layers, where the provided data of validation is received by the input layer, and the competing layer is made up of neurons that compete with one other.

5.3.2. Statistical comparison and error-correction

Through comparing the computed given data with the numerical output results, the error of the output variables can be calculated in many ways. Hence, to evaluate the feasibility of the ANN model of coupled heat and moisture transfers, a statistical analysis between simulated and experimental values can be performed using statistical estimators like the Root Mean Square Error (RMSE) and the coefficient of determination (R^2).

- Root mean square error (RMSE):

The efficiency of the ANN model in representing a given set of measured data can be measured during the learning phase by calculating the RMSE values of the output data:

$$RMSE = \sqrt{\frac{\sum_{i=1}^N (P_i - A_i)^2}{N}}$$

Where P_i is the predicted network output, A_i is the actual measured/experimental data and N is the number of samples in the data set.

- Coefficient of determination (R^2):

The coefficient of determination quantifies the linear relationship between the predictive variable output and the provided calculated data. It is expressed as follows:

$$R^2 = 1 - \frac{SSE}{SST} = \frac{\sum_{i=1}^N (P_i - A_i)^2}{\sum_{i=1}^N (P_i - \bar{A}_i)^2}$$

Where P_i is the predicted network output, A_i is the actual measured/experimental data and \bar{A}_i is their respective average values.

5.4. ANN approach for building energy simulation

Several works from the literature deal with the use of the ANN approach to simulate the thermal behavior of buildings. For instance, Sözer et Aldin [112] and Chegari et al. [113], use ANN to predict the indoor air temperature, but only the three works by Tijskens et al. (2019) [114], (2020) [115] and O. May Tzuc et al. [116] (2021) use ANN to predict the hygrothermal behavior of buildings component.

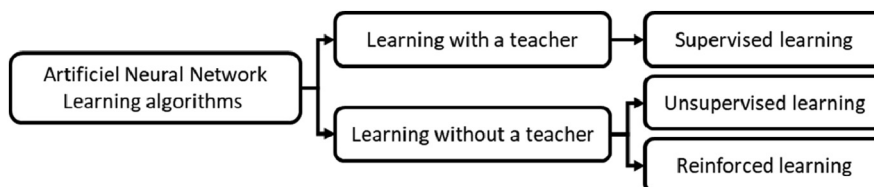


Fig. 10. Different learning method of ANN.

The first study (Table 9) focuses on the application of ANN (multilayer perceptron (MLP) recurrent (RNN) and convolutional networks (CNN)) to predict hygrothermal response time series based on climate data time series. The authors show that only the recurrent (RNN) and convolutional networks (CNN) are able to capture the complex patterns of the hygrothermal response. Additionally, the convolutional network performed significantly better and was 10 times faster to train for the current application example than the recurrent network.

To explore the performance of the different neural networks described above, they are applied to predict the hygrothermal performance of a massive masonry wall in a probabilistic context. The same authors in the second study have done the same work and have applied the same approach of hygrothermal behavior using the ANN method but they have used another type of wall, the timber frame wall [115], instead of the old massive masonry type wall of their previous publication [114].

In the third work, O. May May Tzuc et al. [116], used Artificial Neural Network (ANN) model to estimate the hygrothermal behavior inside a concrete wall protected by a second foliage skin (Table 9). The proposed neural network is trained and tested using a database corresponding to Finland's climatic conditions. 70% of the training experimental data are used to adjust the predictive model to the behavior of the output variables using a guided ANN learning algorithm. During the elaboration of the multi-output model, the complexity of the neural network was mainly determined by the hygrothermal parameter exhibiting the largest difficulty of estimation, i.e. humidity inside the wall. The authors conclude that ANN modeling proved to be an adequate tool that allows researchers to know the behavior inside the concrete, without the need of using variables that are difficult to quantify. We could not find in the literature any use of the ANN approach for the hygrothermal behavior of bio-based materials.

• Strength and weakness of the ANN approach

The performance of a whole building requires a lot of data and highly complex parameterization to cover the entire design space. For example, modelling a three-floor building with varying floor areas and geometries will be difficult to parameterize, and a large number of parameters will make it difficult to find enough representative data. Hence, an ANN approach requires a minimum of inputs which is usually related to outdoor conditions. Consequently, the ANNs are significantly limited by the fact that this implies to have a relevant database. Indeed, it is really important to train the ANN with an exhaustive learning basis with representative and complete samples. Furthermore, it is also difficult to understand the physical phenomena using these models, the hygrothermal behavior change related to the climatic conditions, occupant's behavior, the set-point temperature, ...

However, using ANNs for hygrothermal simulations does not require the knowledge of the materials properties such as sorption, hysteresis, thermal conductivity, specific heat ... but only materials' relative humidity and temperature, global relative humidity (RH), ambient temperature.

Table 9
Summary of building hygrothermal simulation studies based on the ANN approach.

Study	ANN Approach	Building scale			ANN architect	Learning methods	Activation function	Statistical comparison
		Material	Wall	Envelope				
May Tzuc et al. [116]	✓	x	✓	x	Feed-forward networks	Supervised learning with experimental data	Tangent sigmoid function	RMSE/MAPE/R ²
Tijskens et al. [114]	✓	x	✓	x	Feed-Forward/back networks	Supervised/unsupervised learning	Not indicated	RMSE/MAPE/R ²

6. Existing data for validation

The main goal of model validation is to ensure that the model is running properly, including the governing equations and boundary conditions, and the accuracy of the model. An appropriate validation of a hygrothermal simulation model can be divided into three sections: i) to confirm that the physical model is correctly executed by comparing it to the analytical solution, ii) to compare the calculations with other numerical results from the literature and already validated, iii) to simulate the dynamic hygrothermal performances of a building envelope exposed to a real outdoor climate and validating it with experimental results. If the numerical and experimental results are consistent, the model validation of the building envelope element is considered to be accurate.

• Analytical validation

Analytical validation is a precise and efficient validation process, but it can only be used in situations for which the analytical solutions are achievable. The governing equations for multilayer enclosures are strongly nonlinear and coupled to one another, making an empirical solution difficult to achieve. Therefore, it is preferred to validate analytically the coupled heat and moisture model at the one-dimensional scale with existing results, such as the ones provided in the benchmarks of Hagentoft et al.[67].

• Numerical-Numerical Validation

This current validation approach can be classified into several categories. It can be confronted to numerical results from previous research literature [29,30], or it can be a conforming validation of existing simulated results from hygrothermal simulation tools, such as WUFI plus for the nodal approach, or the COMSOL Multiphysics benchmarks for the CFD approach [95]. If we use a programming technique, such as FORTRAN language with difference finite discretization, we may either rely on self-programming results.

• Experimental Validation

Experimenting is still the most efficient and reliable approach to validate coupled heat and moisture transfer models. The reliability of model calculation is determined by comparing computational model outputs to experimental results. Several experiments dealing with model validation have been performed by academics.

The three scales of the building, material, wall, and envelope were divided in recent experimental studies to validate hygrothermal models for building materials and envelopes. Where, the material scale consists of two types of compartments: climate chamber [16,39] and air tunnel [92,117] facilities which can be used to analyze the hygrothermal responses of a single material exposure to controlled conditions, with the only difference being the ability to control convective boundary conditions which exist only for the tunnel dispositive. On the one hand, the wall scale can be categorized to be exposed to either temperature-controlled chamber conditions or natural outside conditions.

The experimental approach to verify the validity of the numerical modeling can be divided into two categories, either to put the wall under a controlled climatic condition [9,13] or to place it under a real environmental condition. This can include single and multi-layer walls and it depends on the case study.

For single and multi-layer walls with hygroscopic materials, Rafidiarison et al. [118] offer sets of experimental data to validate one-dimensional heat and moisture transfer models. Their experimental tests were carried out in a double climate chamber of simple to complex climate conditions with oscillation cycles. Their study results can be used to verify any hygrothermal computational simulation's reliability.

7. Conclusion

For this study, we developed a methodology that could be used by other researchers. No studies, however, provided detailed lighting hygrothermal behavior simulation methods of hygroscopic buildings. Therefore, the presented outcome can be very helpful for energy modelers and decision makers to better understand the building performance analysis through benchmarking and can help in estimating the real impact of moisture transfer on thermal comfort. The strength of this study includes the use of completing, detailed of a physical and data driven models as well as the advantage and limitation of each model. Our findings contribute to literature on hygrothermal simulation methods in the residential hygroscopic building sector.

The majority of numerical approaches have been examined and proven to be capable of producing reliable findings. It is important to remember that the simulations make allowances for extremely difficult situations of non-linear interaction and dynamics. Due to a variation in the computing techniques, the outputs may vary from one simulation to another. The numerical scheme, the algorithm for solving the equations, the mesh size and the boundary conditions with various sets of potential inputs are examples of these influencing parameters.

The proper simulation of the hygrothermal behavior of hygroscopic building materials is a challenging task, which may influence the suitability of retrofit strategies complying general thermal regulations. Indeed, an incorrect simulation can lead to inadequate conclusions, which might lead to improper actions when renovating buildings for more energy efficiency. This review highlights a significant gap of actual building energy simulation software's for computing the combined heat and moisture transfer phenomena. It reveals that the majority of the softwares simplify the computing methods by neglecting envelope moisture buffering, which contributes to incorrect energy simulations.

Several models are used to simulate the hygrothermal behavior of buildings based on hygroscopic materials, which belong to two types:

- White-box models which are based on physical knowledge of the building and hygrothermal balance equations. These are often obtained through energy simulation software such as COMSOL Multiphysics or WUFI.
- Black-box models which use only measured input/output data and statistical estimation methods such as ANN, CNN and LSTM models.

However, each technique has its advantages and inconveniences. The White-box models are divided into two sub-categories:

- The CFD approach which describes each zone in several control volumes.

- The nodal approach, which treats each specified zone as a homogeneous volume with uniform physical variables.

In some cases, the benefits provided by one tool are missing in the other tool, such that an 'optimum' model would be the combination of both tools, requiring a coupling strategy. For this purpose, we have listed the studies that were effective in achieving a co-simulation between two different softwares that account for coupled heat and moisture transfers at different building scales. The review shows that there is a need for a well-known method to determine the hygrothermal boundary conditions for materials and/or building scales.

We can find in the literature some analytical approaches to describe the hygrothermal behavior of hygroscopic materials, but this still does not reflect the real complexity of time-varying outdoor humidity, temperature, and incident solar radiation. The significant limitation of these approaches is that they lack the integration of the complexity of real-life buildings, in which multiple heat and mass fluxes are present.

We also have included in this paper the methods based on machine learning (black box methods), which rely on statistical treatments of building hygrothermal behavior. Several neural network models have been tested in the literature such as: The basic structure of an Artificial neural networks (ANN), multilayer perceptron (MLP) recurrent (RNN) and convolutional networks (CNN). These methods are particularly useful in circumstances where material and envelope physical properties, as well as geometry, are unavailable. Machine learning modeling need less knowledge about the building than physical modeling and can tend to be easier to implement.

In conclusion, the information collected in this work provides guidance to researchers and engineers involved in building simulations and can lead to design and rehabilitation studies of hygroscopic building materials. As can be seen, the literature is not unanimous on the relevance of hygrothermal behavior of buildings based on hygroscopic materials (bio-based materials for example). There is no extensive study on the hygrothermal behavior simulation of an entire building based on a hygroscopic material taking into account the occupants and the HVAC systems. The studies were limited to the wall scale. Furthermore, the literature review indicates a knowledge gap on hygrothermal bridges for a building based on a hygroscopic material.

Declaration of Competing Interest

The authors declare that they have no known competing financial interests or personal relationships that could have appeared to influence the work reported in this paper.

References

- [1] United Nations and Department of Economic and Social Affairs. Energy statistics pocketbook 2020. 2020.
- [2] World Commission on Environment and Development, *Our Common Future*, Oxford University Press, Oxford, 1987.
- [3] United Nations, *United Nations Framework Convention on Climate Change*, United Nations, General Assembly, New York, 1992.
- [4] "Montreal Protocol on Substances that Deplete the Ozone Layer. Montreal, Sep. 16, 1987.
- [5] "Kyoto Protocol to the United Nations Framework Convention on Climate Change. Japon, Dec. 11, 1997. [Online]. Available: %20http://unfccc.int/resource/docs/cop3/07a01.pdf
- [6] "History of the Convention | UNFCCC." <https://unfccc.int/process/the-convention/history-of-the-convention#eq-2> (accessed Feb. 03, 2021).
- [7] Eurostat. Energy statistics – quantities. Eur. Comm. Database, 2020. [Online]. Available: <https://ec.europa.eu/eurostat/en/web/main/data/database>
- [8] Eurostat. Energy consumption and use by households. Eur. Comm. Database, 2020. [Online]. Available: https://ec.europa.eu/eurostat/statistics-explained/index.php?title=Energy_consumption_in_households

- [9] J. Berger, W. Mazuroski, N. Mendes, S. Guernouti, M. Woloszyn, 2D whole-building hygrothermal simulation analysis based on a PGD reduced order model, *Energy Build.* 112 (Jan. 2016) 49–61, <https://doi.org/10.1016/j.enbuild.2015.11.023>.
- [10] H.J. Steeman, A. Janssens, J. Carmeliet, M.D. Paepe, Modelling indoor air and hygrothermal wall interaction in building simulation: Comparison between CFD and a well-mixed zonal model, *Build. Environ.* (2009) 12.
- [11] M. Rahim, Numerical investigation of the effect of non-isotherme sorption characteristics on hygrothermal behavior of two bio-based building walls, *J. Build. Eng.* (2016) 10.
- [12] B. Seng, Scale analysis of heat and moisture transfer through bio-based materials – Application to hemp concrete, *Energy Build.* (2017) 13.
- [13] T. Colinart, Temperature dependence of sorption isotherm of hygroscopic building materials. Part 2: Influence on hygrothermal behavior of hemp concrete, *Energy Build.* (2017) 10.
- [14] B. Moujalled, Y. Ait Ouméziane, S. Moissette, M. Bart, C. Lanos, D. Samri, Experimental and numerical evaluation of the hygrothermal performance of a hemp lime concrete building: A long term case study, *Build. Environ.* 136 (May 2018) 11–27, <https://doi.org/10.1016/j.buildenv.2018.03.025>.
- [15] G. Promis, O. Douzane, A.D. Tran Le, T. Langlet, “Moisture hysteresis influence on mass transfer through bio-based building materials in dynamic state”, *May, Energy Build.* 166 (2018) 450–459, <https://doi.org/10.1016/j.enbuild.2018.01.067>.
- [16] T. Alioua, B. Agoudjil, N. Chennouf, A. Boudenne, K. Benzarti, Investigation on heat and moisture transfer in bio-based building wall with consideration of the hysteresis effect, *Build. Environ.* 163 (2019) 106333, <https://doi.org/10.1016/j.buildenv.2019.106333>.
- [17] P. Huang et al., Heat and moisture transfer behaviour in *Phyllostachys edulis* (Moso bamboo) based panels, *Constr. Build. Mater.* (2018) 15.
- [18] M. Khoukhi, The combined effect of heat and moisture transfer dependent thermal conductivity of polystyrene insulation material: Impact on building energy performance, *Energy Build.* 169 (Jun. 2018) 228–235, <https://doi.org/10.1016/j.enbuild.2018.03.055>.
- [19] J. M. P. Q. Delgado, E. Barreira, N. M. M. Ramos, and V. P. de Freitas, *Hygrothermal Numerical Simulation Tools Applied to Building Physics*, Berlin, Heidelberg: Springer Berlin Heidelberg, 2013. doi: 10.1007/978-3-642-35003-0.
- [20] J.R. Philip, D.A. De Vries, Moisture movement in porous materials under temperature gradients, *Trans. Am. Geophys. Union* 38 (2) (1957) 222, <https://doi.org/10.1029/TR038i002p00222>.
- [21] S. Whitaker, Simultaneous Heat, Mass, and Momentum Transfer in Porous Media: A Theory of Drying, in *Advances in Heat Transfer*. 13. Elsevier. 1977. 119–203. doi: 10.1016/S0065-2717(08)70223-5.
- [22] A.V. luikov, Application of irreversible thermodynamics methods to investigation of heat and mass transfer, *Int. J. Heat Mass Transf.* 9 (1966) 139–152.
- [23] H.M. Künzle, Simultaneous heat and moisture transport in building components: one- and two-dimensional calculation using simple parameters, IRB-Verl, Stuttgart, 1995.
- [24] N. Mendes, I. Ridley, R. Lamberts, P.C. Philippi, K. Budag, UMIDUS: A PC program for the prediction of heat and moisture transfer in porous buildings elements, *Build. Simul.* (1999) 277–283.
- [25] M.H. Benzaama, L.H. Rajaorasoa, B. Ajib, S. Lecoche, A data-driven methodology to predict thermal behavior of residential buildings using piecewise linear models, *J. Build. Eng.* 32 (2020) 101523, <https://doi.org/10.1016/j.job.2020.101523>.
- [26] S. A. Klein et al. TRAnsient SYstem Simulation program 18: Programme's Guide." 2017. [Online]. Available: <https://sel.me.wisc.edu/trnsys/user18-resources/index.html>
- [27] P. LENORMAND et al. Manuel Comfie Pleiades Modeleur." Izuba énergies. [Online]. Available: https://docs.izuba.fr/v4/fr/index.php/Pleiades_et_ses_modules
- [28] H. Künzle, K. Kiesel, Calculation of heat and moisture transfer in exposed building components, *Int. J. Heat Mass Transf.* 40 (1) (1997) 159–167.
- [29] N. Mendes, P.C. Philippi, A method for predicting heat and moisture transfer through multilayered walls based on temperature and moisture content gradients, *Int. J. Heat Mass Transf.* (2005) 15.
- [30] N. Mendes, P.C. Philippi, R. Lamberts, A new mathematical method to solve highly coupled equations of heat and mass transfer in porous media, *Int. J. Heat Mass Transf.* 45 (3) (Jan. 2002) 509–518, [https://doi.org/10.1016/S0017-9310\(01\)00172-7](https://doi.org/10.1016/S0017-9310(01)00172-7).
- [31] S.-H. Cho and C.-U. Chae, A Study on Life Cycle CO₂ Emissions of Low-Carbon Building in South Korea. *Sustainability*, vol. 8, no. 6, Art. no. 6, Jun. 2016, doi: 10.3390/su8060579.
- [32] H. Dahy, Biocomposite materials based on annual natural fibres and biopolymers – Design, fabrication and customized applications in architecture, *Constr. Build. Mater.* 147 (Aug. 2017) 212–220, <https://doi.org/10.1016/j.conbuildmat.2017.04.079>.
- [33] G. Bumanis, L. Vitola, I. Pundiene, M. Sinka, and D. Bajare, Gypsum, Geopolymers, and Starch—Alternative Binders for Bio-Based Building Materials: A Review and Life-Cycle Assessment. *Sustainability*, vol. 12, no. 14, Art. no. 14, Jul. 2020, doi: 10.3390/su12145666.
- [34] X. Zhang, M. Riaz Ahmad, and B. Chen, Numerical and experimental investigation of the hygrothermal properties of corn stalk and magnesium phosphate cement (MPC) based bio-composites. *Constr. Build. Mater.*, vol. 244, p. 118358, May 2020, doi: 10.1016/j.conbuildmat.2020.118358.
- [35] N. Reuge, Modeling of hygrothermal transfers through a bio-based multilayered wall tested in a bi-climatic room, *J. Build. Eng.* (2020) 12.
- [36] M. Bagarić, I. Banjad Pečur, and B. Milovanović, Hygrothermal performance of ventilated prefabricated sandwich wall panel from recycled construction and demolition waste – A case study. *Energy Build.*, vol. 206, p. 109573, Jan. 2020, doi: 10.1016/j.enbuild.2019.109573.
- [37] W. Dong, Y. Chen, Y. Bao, A. Fang, A validation of dynamic hygrothermal model with coupled heat and moisture transfer in porous building materials and envelopes, *J. Build. Eng.* 32 (2020) 101484, <https://doi.org/10.1016/j.job.2020.101484>.
- [38] A. Tadeu, L. Škerget, N. Simões, R. Fino, Simulation of heat and moisture flow through walls covered with uncoated medium density expanded cork, *Build. Environ.* 142 (Sep. 2018) 195–210, <https://doi.org/10.1016/j.buildenv.2018.06.009>.
- [39] S. Hou, F. Liu, S. Wang, H. Bian, Coupled heat and moisture transfer in hollow concrete block wall filled with compressed straw bricks, *Energy Build.* 135 (Jan. 2017) 74–84, <https://doi.org/10.1016/j.enbuild.2016.11.026>.
- [40] G.B.A. Coelho, H.E. Silva, F.M.A. Henriques, Calibrated hygrothermal simulation models for historical buildings, *Build. Environ.* 142 (Sep. 2018) 439–450, <https://doi.org/10.1016/j.buildenv.2018.06.034>.
- [41] D. Gallipoli, A. W. Bruno, C. Perlot, and J. Mendes, “A geotechnical perspective of raw earth building. *Acta Geotech.*, vol. 12, no. 3, Art. no. 3, Jun. 2017, doi: 10.1007/s11440-016-0521-1.
- [42] N.N. Makhlof, D. Maskell, A. Marsh, S. Natarajan, M. Dabaieh, M.M. Afify, Hygrothermal performance of vernacular stone in a desert climate, *Constr. Build. Mater.* 216 (Aug. 2019) 687–696, <https://doi.org/10.1016/j.conbuildmat.2019.04.244>.
- [43] L. Boukhattem, M. Boumhaout, H. Hamdi, B. Benhamou, and F. Ait Nouh, Moisture content influence on the thermal conductivity of insulating building materials made from date palm fibers mesh. *Constr. Build. Mater.*, vol. 148, pp. 811–823, Sep. 2017, doi: 10.1016/j.conbuildmat.2017.05.020.
- [44] M.G. Gomes, I. Flores-Colen, L.M. Manga, A. Soares, J. de Brito, The influence of moisture content on the thermal conductivity of external thermal mortars, *Constr. Build. Mater.* 135 (Mar. 2017) 279–286, <https://doi.org/10.1016/j.conbuildmat.2016.12.166>.
- [45] P.M. Congedo, C. Baglivo, D. D'Agostino, G. Quarta, P. Di Gloria, Rising damp in building stones: Numerical and experimental comparison in leccese stone and carparo under controlled microclimatic conditions, *Constr. Build. Mater.* 296 (2021) 123713, <https://doi.org/10.1016/j.conbuildmat.2021.123713>.
- [46] H.E. Huerto-Cardenas, F. Leonforte, N. Aste, C. Del Pero, G. Evola, V. Costanzo, E. Lucchi, Validation of dynamic hygrothermal simulation models for historical buildings: State of the art, research challenges and recommendations, *Build. Environ.* 180 (2020) 107081, <https://doi.org/10.1016/j.buildenv.2020.107081>.
- [47] N. Cavalagli, A. Kita, V.L. Castaldo, A.L. Pisello, F. Ubertini, Hierarchical environmental risk mapping of material degradation in historic masonry buildings: An integrated approach considering climate change and structural damage, *Constr. Build. Mater.* 215 (Aug. 2019) 998–1014, <https://doi.org/10.1016/j.conbuildmat.2019.04.204>.
- [48] C. Franzen, P.W. Mirwald, Moisture sorption behaviour of salt mixtures in porous stone, *Geochemistry* 69 (1) (Feb. 2009) 91–98, <https://doi.org/10.1016/j.chemer.2008.02.001>.
- [49] D. D'Agostino, P.M. Congedo, CFD modeling and moisture dynamics implications of ventilation scenarios in historical buildings, *Build. Environ.* 79 (Sep. 2014) 181–193, <https://doi.org/10.1016/j.buildenv.2014.05.007>.
- [50] D. D'Agostino, P.M. Congedo, R. Cataldo, Computational fluid dynamics (CFD) modeling of microclimate for salts crystallization control and artworks conservation, *J. Cult. Herit.* 15 (4) (Jul. 2014) 448–457, <https://doi.org/10.1016/j.culher.2013.10.002>.
- [51] F. Corvo, J. Reyes, C. Valdes, F. Villaseñor, O. Cuesta, D. Aguilar, P. Quintana, Influence of Air Pollution and Humidity on Limestone Materials Degradation in Historical Buildings Located in Cities Under Tropical Coastal Climates, *Water, Air, Soil Pollut.* 205 (1–4) (2010) 359–375, <https://doi.org/10.1007/s11270-009-0081-1>.
- [52] M. Cellura, F. Guarino, S. Longo, G. Tumminia, Climate change and the building sector: Modelling and energy implications to an office building in southern Europe, *Energy Sustain. Dev.* 45 (Aug. 2018) 46–65, <https://doi.org/10.1016/j.esd.2018.05.001>.
- [53] C.M. Grossi, P. Brimblecombe, I. Harris, Predicting long term freeze-thaw risks on Europe built heritage and archaeological sites in a changing climate, *Sci. Total Environ.* 377 (2) (May 2007) 273–281, <https://doi.org/10.1016/j.scitotenv.2007.02.014>.
- [54] C.R. Pedersen, Prediction of moisture transfer in building constructions, *Build. Environ.* 27 (3) (Jul. 1992) 387–397, [https://doi.org/10.1016/0360-1323\(92\)90038-Q](https://doi.org/10.1016/0360-1323(92)90038-Q).
- [55] H.D. Baehr, K. Stephan, *Mass transfer Theory*, in: *Heat and Mass Transfer*, Springer, Berlin, Heidelberg, 2011, pp. 87–102, <https://doi.org/10.1007/978-3-642-20021-2>.
- [56] D. Lelievre, T. Colinart, P. Glouannec, Hygrothermal behavior of bio-based building materials including hysteresis effects: Experimental and numerical analyses, *Energy Build.* 84 (Dec. 2014) 617–627, <https://doi.org/10.1016/j.enbuild.2014.09.013>.
- [57] J.-P. Hansen, *Theory of Simple Liquids with Applications to Soft Matter*, 4th ed., Academic Press, Oxford, England, 2013.

- [58] H. Swenson and N. P. Stadie. Langmuir's Theory of Adsorption: A Centennial Review. *Langmuir*, vol. 35, no. 16, Art. no. 16, Apr. 2019, doi: 10.1021/acs.langmuir.9b00154.
- [59] S. Brunauer, P. H. Emmett, and E. Teller. Adsorption of Gases in Multimolecular Layers. *J. Am. Chem. Soc.*, vol. 60, no. 2, Art. no. 2, Feb. 1938, doi: 10.1021/ja01269a023.
- [60] M. Labat, M. Woloszyn, G. Garnier, J.J. Roux, Dynamic coupling between vapour and heat transfer in wall assemblies: Analysis of measurements achieved under real climate, *Build. Environ.* 87 (May 2015) 129–141, <https://doi.org/10.1016/j.buildenv.2015.01.022>.
- [61] M. Van Belleghem, H.-J. Steeman, M. Steeman, A. Janssens, M. De Paep, Sensitivity analysis of CFD coupled non-isothermal heat and moisture modelling, *Build. Environ.* 45 (11) (Nov. 2010) 2485–2496, <https://doi.org/10.1016/j.buildenv.2010.05.011>.
- [62] M. Steeman, A. Janssens, H.J. Steeman, M.V. Belleghem, M.D. Paep, On coupling 1D non-isothermal heat and mass transfer in porous materials with a multizone building energy simulation model, *Build. Environ.* (2010) 13.
- [63] S. CHAPMAN and T. G. COWLING. The Free Path, the collision-frequency and persistence of velocities. In *The mathematical theory of non-uniform gases: An account of the kinetic theory of viscosity, thermal conduction and diffusion in gases*, 1953, pp. 89–99.
- [64] M. G. Verbeek. A Numerical Investigation of the Mean Free Path Distribution in the Knudsen Regime. *Transp. Porous Media*, vol. 123, no. 2, Art. no. 2, Jun. 2018, doi: 10.1007/s11242-018-1035-0.
- [65] H.D. Baehr, K. Stephan, *The different types of heat transfer*, in: *Heat and Mass Transfer*, Springer, Berlin, Heidelberg, 2011, pp. 1–27, <https://doi.org/10.1007/978-3-642-20021-2>.
- [66] R. Karwa, *Mass Transfer*, in: *Heat and Mass Transfer*, Springer Singapore, Singapore, 2020, pp. 1041–1064, <https://doi.org/10.1007/978-981-15-3988-6>.
- [67] C.-E. Hagentoft, A. S. Kalagasidis, and B. Adl-Zarrabi. Benchmarks for One-dimensional Cases of Combined Heat, Air and Moisture Transfer in Building Components. p. 10.
- [68] G.A. Nagata, T.V. Costa, M.T.B. Perazzini, H. Perazzini, Coupled heat and mass transfer modelling in convective drying of biomass at particle-level: Model validation with experimental data, *Renew. Energy* 149 (Apr. 2020) 1290–1299, <https://doi.org/10.1016/j.renene.2019.10.123>.
- [69] D. Zirkelbach, T. Schmidt, M. Kehr, and H. M. Künzel. WUFI Pro 5 Manual." [Online]. Available: <https://wufi.de/en/service/downloads/>
- [70] A. D. Tran Le, J. S. Zhang, and Z. Liu. Impact of humidity on formaldehyde and moisture buffering capacity of porous building material. *J. Build. Eng.*, vol. 36, p. 102114, Apr. 2021, doi: 10.1016/j.jobee.2020.102114.
- [71] R. Wang. Moisture-safe attic design in extremely cold climate: Hygrothermal simulations. *Build. Environ.*, p. 12, 2020.
- [72] "EnergyPlus™ Version 9.4.0 Documentation: Engineering Reference. US Department Energy, p. 1758, Sep. 2020.
- [73] F. Antretter, M. Winkler, M. Fink, M. Pazold, J. Radon, and S. S. Stadler. WUFI Plus 3.1 Manual." Jun. 01, 2017. [Online]. Available: <https://wufi.de/en/service/downloads/>
- [74] R. Djedjig, E. Bozonnet, R. Belarbi, Analysis of thermal effects of vegetated envelopes: Integration of a validated model in a building energy simulation program, *Energy Build.* 86 (Jan. 2015) 93–103, <https://doi.org/10.1016/j.enbuild.2014.09.057>.
- [75] J. Preuss. Moisture Balance. in *TRAnsient SYstem Simulation program 18: Multizone Building modeling with Type56 and TRNBuild*, TRNSYS, pp. 191–195.
- [76] "Effective Moisture Penetration Depth (EMPD) Model. in *EnergyPlus™ Version 9.4.0 Documentation: Engineering Reference*, US Department of Energy, 2020, pp. 80–83.
- [77] M.H. Benzaama, A.M. Mokhtari, M. Lachi, C. Maalouf, S. Menhoudj, Sunspot analysis under varying conditions climate: Distributed radiation on cooling floor and its effect on dynamic thermal behaviour, *Sol. Energy* 221 (Jun. 2021) 275–291, <https://doi.org/10.1016/j.solener.2021.03.082>.
- [78] A. Kerestecioglu and A. Kamel. Theoretical and computational investigation of simultaneous heat and moisture transfer in buildings: 'Effective penetration depth' theory. 1989. Accessed: Apr. 05, 2021. [Online]. Available: <https://www.aivc.org/resource/theoretical-and-computational-investigation-simultaneous-heat-and-moisture-transfer>
- [79] J. Woods, J. Winkler, and D. Christensen. Moisture Modeling: Effective Moisture Penetration Depth Versus Effective Capacitance. p. 13.
- [80] T. Yamamoto, A. Ozaki, M. Lee, H. Kusumoto, Fundamental study of coupling methods between energy simulation and CFD, *Energy Build.* 159 (Jan. 2018) 587–599, <https://doi.org/10.1016/j.enbuild.2017.11.059>.
- [81] M. Simo-Tagne, M.C. Ndukwu, Y. Rogaume, Modelling and numerical simulation of hygrothermal transfer through a building wall for locations subjected to outdoor conditions in Sub-Saharan Africa, *J. Build. Eng.* 26 (2019) 100901, <https://doi.org/10.1016/j.jobee.2019.100901>.
- [82] Y. Kang, S.J. Chang, S. Kim, Hygrothermal behavior evaluation of walls improving heat and moisture performance on gypsum boards by adding porous materials, *Energy Build.* 165 (Apr. 2018) 431–439, <https://doi.org/10.1016/j.enbuild.2017.12.052>.
- [83] M. Qin, R. Belarbi, A. Ait-Mokhtar, L.-O. Nilsson, Coupled heat and moisture transfer in multi-layer building materials, *Constr. Build. Mater.* (2009) 9.
- [84] ANSYS, Inc. *Heat Transfer*. in *ANSYS Fluent Theory Guide: Release 15.0*, 2013, pp. 133–173.
- [85] "OpenFoam : User Guide version 8. Aug. 22, 2020. <https://cfd.direct/openfoam/user-guide/>
- [86] Siemens PLM Software. STAR-CCM+ Documentation Version 13.04." 2018.
- [87] "Comsol Multiphysics 5.6 : Porous Media Flow Module User's Guide." [Online]. Available: <https://doc.comsol.com/5.6/docserver/pdf/com.comsol.help.comsol/helpdesk/helpdesk.html>
- [88] Z. Zhai, Q. Chen, P. Haves, J.H. Klems, On approaches to couple energy simulation and computational uid dynamics programs, *Build. Environ.* (2002) 8.
- [89] Z. J. Zhai and Q. Y. Chen. Performance of coupled building energy and CFD simulations. *Energy Build.*, vol. 37, no. 4, Art. no. 4, Apr. 2005, doi: 10.1016/j.enbuild.2004.07.001.
- [90] H. Zhang, Investigating simultaneous transport of heat and moisture in hygroscopic materials by a semi-conjugate CFD-coupled approach, *Build. Environ.* (2015) 11.
- [91] Q. Li, J. Rao, P. Fazio, Development of HAM tool for building envelope analysis, *Build. Environ.* (2009) 9.
- [92] H.-J. Steeman, M. Van Belleghem, A. Janssens, M. De Paep, Coupled simulation of heat and moisture transport in air and porous materials for the assessment of moisture related damage, *Build. Environ.* 44 (10) (Oct. 2009) 2176–2184, <https://doi.org/10.1016/j.buildenv.2009.03.016>.
- [93] Q. Li, J. Rao, and P. Fazio. Hygrothermal simulation of drying performance of typical north american building envelope. Montréal, Canada, 18/08 2005, p. 8.
- [94] L. Škerget, A. Tadeu, C.A. Brebbia, Transient simulation of coupled heat and moisture flow through a multi-layer porous solid exposed to solar heat flux, *Int. J. Heat Mass Transf.* 117 (2018) 273–279, <https://doi.org/10.1016/j.ijheatmasstransfer.2017.10.010>.
- [95] "Comsol Multiphysics 5.6: Heat and Moisture Transport in a Semi-Infinite Wall." [Online]. Available: <https://www.comsol.fr/model/heat-and-moisture-transport-in-a-semi-infinite-wall-39001>
- [96] Guggenheim Edward Armand, *Applications of statistical mechanics*, by E.A. Clarendon Press, Guggenheim, Oxford, 1966.
- [97] R.B. Anderson, Modifications of the Brunauer, Emmett and Teller Equation 1, *J. Am. Chem. Soc.* 68 (4) (Apr. 1946) 686–691, <https://doi.org/10.1021/ja01208a049>.
- [98] Boer Jan Hendrik de, *The dynamical character of adsorption*, by J. H. de Boer. Oxford: Clarendon Press, 1953.
- [99] I. Langmuir, The adsorption of gases on plane surfaces of glass, mica and platinum, *J. Am. Chem. Soc.* 40 (9) (Sep. 1918) 1361–1403, <https://doi.org/10.1021/ja02242a004>.
- [100] M.T. van Genuchten, A Closed-form Equation for Predicting the Hydraulic Conductivity of Unsaturated Soils, *Soil Sci. Soc. Am. J.* 44 (5) (1980) 892–898, <https://doi.org/10.2136/sssaj1980.03615995004400050002x>.
- [101] M. Maaroufi, Experimental and numerical highlighting of water vapor sorption hysteresis in the coupled heat and moisture transfers, *J. Build. Eng.* (2021) 10.
- [102] Y. Muallem, A conceptual model of hysteresis, *Water Resour. Res.* 10 (3) (1974) 514–520, <https://doi.org/10.1029/WR010i003p00514>.
- [103] C. Rode, P. N. Hansen, and K. K. Hansen. Combined heat and moisture transfer in building constructions. pp. 42–44, 1990.
- [104] J.B. Kool, J.C. Parker, Development and evaluation of closed-form expressions for hysteretic soil hydraulic properties, *Water Resour. Res.* 23 (1) (1987) 105–114, <https://doi.org/10.1029/WR023i001p0105>.
- [105] H.-C. Huang, Y.-C. Tan, C.-W. Liu, C.-H. Chen, A novel hysteresis model in unsaturated soil, *Hydrol. Process.* 19 (8) (2005) 1653–1665, [https://doi.org/10.1002/\(ISSN\)1099-108510.1002/hyp.v19:810.1002/hyp.5594](https://doi.org/10.1002/(ISSN)1099-108510.1002/hyp.v19:810.1002/hyp.5594).
- [106] Y. A. Oumeziane, M. Bart, S. Moissette, and C. Lanos. Hysteretic Behaviour and Moisture Buffering of Hemp Concrete. p. 19.
- [107] K.-T. Yang. Artificial Neural Networks (ANNs): A New Paradigm for Thermal Science and Engineering. *J. Heat Transf.*, vol. 130, no. 093001, Jul. 2008, doi: 10.1115/1.2944238.
- [108] L. V. Kamble, D. R. Pangavhane, and T. P. Singh. Heat Transfer Studies using Artificial Neural Network – a Review. p. 18, 2014.
- [109] A. K. Jain, Jianchang Mao, and K. M. Mohiuddin. Artificial neural networks: a tutorial. *Computer*, vol. 29, no. 3, pp. 31–44, Mar. 1996, doi: 10.1109/2.485891.
- [110] I. Livshin. Learning About Neural Networks. in *Artificial Neural Networks with Java: Tools for Building Neural Network Applications*, Apress, 2019, pp. 3–4. doi: 10.1007/978-1-4842-4421-0.
- [111] S. Haykin. *Learning Processes*. in *Neural networks and learning machines*, 3. ed., New York: Pearson, 2009, pp. 34–44
- [112] H. Sözer, S.S. Aldin, Predicting the indoor thermal data for heating season based on short-term measurements to calibrate the simulation set-points, *Energy Build.* 202 (2019) 109422, <https://doi.org/10.1016/j.enbuild.2019.109422>.
- [113] B. Chegari, M. Tabaa, E. Simeu, F. Moutaouakkil, H. Medromi, Multi-objective optimization of building energy performance and indoor thermal comfort by combining artificial neural networks and metaheuristic algorithms, *Energy Build.* 239 (2021) 110839, <https://doi.org/10.1016/j.enbuild.2021.110839>.
- [114] A. Tijsskens, S. Roels, H. Janssen, Neural networks for metamodeling the hygrothermal behaviour of building components, *Build. Environ.* 162 (2019) 106282, <https://doi.org/10.1016/j.buildenv.2019.106282>.
- [115] A. Tijsskens, S. Roels, H. Janssen, Hygrothermal assessment of timber frame walls using a convolutional neural network, *Build. Environ.* 193 (2021) 107652, <https://doi.org/10.1016/j.buildenv.2021.107652>.

- [116] O. May Tzuc et al. Modeling of hygrothermal behavior for green facade's concrete wall exposed to nordic climate using artificial intelligence and global sensitivity analysis. *J. Build. Eng.*, vol. 33, p. 101625, Jan. 2021, doi: 10.1016/j.jobbe.2020.101625.
- [117] M. Van Belleghem, M. Steeman, H. Janssen, A. Janssens, M. De Paepe, Validation of a coupled heat, vapour and liquid moisture transport model for porous materials implemented in CFD. *Build. Environ.* 81 (2014) 340–353, <https://doi.org/10.1016/j.buildenv.2014.06.024>.
- [118] H. Rafidiarison, Dataset for validating 1-D heat and mass transfer models within building walls with hygroscopic materials, *Build. Environ.* (2015) 13.